In presenting the dissertation as a partial fulfillment of the requirements for an advanced degree from the Georgia Institute of Technology, I agree that the Library of the Institute shall make it available for inspection and circulation in accordance with its regulations governing materials of this type. I agree that permission to copy from, or to publish from, this dissertation may be granted by the professor under whose direction it was written, or, in his absence, by the Dean of the Graduate Division when such copying or publication is solely for scholarly purposes and does not involve potential financial gain. It is understood that any copying from, or publication of, this dissertation which involves potential financial gain will not be allowed without written permission.

_____

_____

7/25/68

VEHICLE CONTROL

BY COUNTING

A THESIS

Presented to

The Faculty of the Graduate Division

by

Variddhi Ungbhakorn

In Partial Fulfillment

of the Requirements for the Degree

Master of Science in Mechanical Engineering

Georgia Institute of Technology

December, 1969

VEHICLE CONTROL

BY COUNTING

Approved: [redacted]

Date approved by Chairman: 12/14/69

ACKNOWLEDGMENTS

I am deeply indebted to Dr. S. L. Dickerson, my thesis advisor, for his knowledgeable guidance and many hours of hard work in helping me complete this thesis.

Appreciation is also extended to Dr. L. A. Holliman and Dr. John B. Peatman, members of the reading committee, for their interest and participation in this research effort.

I would also like to thank Mr. Chris H. Bartlett, Vice President of Westinghouse Electric Corporation, Mrs. Virginia S. Berghund, and Mr. Earl W. Nelson, Chief Engineer of Metropolitan Atlanta Rapid Transit Authority, for their help in the information about the "skybus."

TABLE OF CONTENTS

LIST OF TABLES

LIST OF ILLUSTRATIONS

LIST OF ILLUSTRATIONS (Continued)

NOMENCLATURE

Actual System		Normalized System		Description
Symbol	Unit	Symbol	Measure Formula	
A	$in.^2$	-	-	Projected area of the vehicle
D	in.	d	L	Marker spacing
E	pulse	e	T	Error in pulses
F(t)	lb	f(t)	L	Net force applied to the vehicle
$F_c(t)$	lb	$f_e(t)$	L	Dynamic control force
$F_d(t)$	lb	$f_d(t)$	L	Disturbing force
$F_W(t)$	lb	-	-	Winddrag force
K	lb/pulse	k	L	Controller gain
$P_E(t)$	pulses/sec	$P_e(t)$	-	Difference in pulse rate
$P_R(t)$	pulses/sec	$P_r(t)$	-	Reference clock pulse rate
$P_V(t)$	pulses/sec	$P_v(t)$	-	Pulse train within the vehicle
T	sec.	-	-	Time constant
V(t)	in./sec.	v(t)	L	Velocity
$\dot{V}(t)$	$in./sec^2$	$\overset{+}{v}(t)$	L	Acceleration
Y(t)	in.	y(t)	L	Distance error
Y_{max}	in.	y_{max}	L	Maximum distance error
Y_{SS}	in.	y_{SS}	L	Steady state error
c	lb-sec/in	-	-	Steady state drag coefficient

NOMENCLATURE (Continued)

Actual System		Normalized System		Description
Symbol	Unit	Symbol	Measure Formula	
g	386 in./sec^2	-	-	Gravitational constant
t	sec	τ	-	time
σ	lb-sec^2/in.^{4}	-	-	Mass density of air
Ω_d	rad./sec	ω_d	-	Damped natural frequency
Ω_n	rad./sec	ω_n	-	Natural frequency
-	-	ξ	-	Damping ratio

SUMMARY

In this study the available control theory is used to design a linear feedback system which regulates the position and velocity of moving vehicles. The system generates its error signals by counting positively clock pulses and negatively wayside markers. Inputs considered are the disturbing force and marker spacings. For step inputs, the static and dynamics errors and characteristics of the system are investigated. The mathematical model is presented. The non-linear system is simulated on an analog computer and the results are compared to predict the range of applicability and accuracy of the linear system.

Results from analytical solutions showed that as the damping ratios increased the steady state error also increased and the overshoots decreased. The results showed that the speed of response was dependent on the ratios of controller gain to marker spacing. The higher values of this ratio resulted in quicker speed of response and lower steady state error but a more oscillatory response was obtained. For a step change in marker spacing the response would show overshoots or undershoots depending on whether the step was down or up. Damping ratios were decreased for a step-down change in marker spacing. The overshoots were increased but the distance error was decreased. The reverse was true for a step-up change in marker spacing.

The simulation results showed that the linear response gave a good approximation to the non-linear one at low values of marker spacing and controller gain.

At high damping ratios the speed of response of the linear system was slower than the non-linear one. The transient responses of the two systems died out rapidly.

The selection of the range of applicability of the problem was based on high speed of response, low sudden acceleration or deceleration, small overshoots or undershoots, and the accuracy of approximation of the linear to the non-linear system. The desired range was the damping ratios of 0.50 to 0.80 with the corresponding ratios of marker spacing to controller gain of 1 to 2.56 and a step change in marker spacing of 30 per cent.

CHAPTER I

INTRODUCTION

Previous Development in Traffic Control Application

Computer-controlled traffic networks have taken hold, as is apparent from the operational system in Toronto, San Jose, Wichita Falls [1]. The machine determines both the volume and average speed of traffic on all streets within the control area and utilizes these data to provide optimum timing at any signal most likely to attain the through movement of vehicles with a minimum of involuntary stops. If the speed of vehicles could be controlled nearest to the desired value during each interval of traffic load, while applying the computer controlled traffic networks, probably the flow of traffic may be improved. W. S. Levine and M. Athans [2] used the theory of optimal control to design an optimal linear feedback system which regulated the position and velocity of vehicles in a densely packed string of high-speed moving vehicles. The design method yielded a good control system. However, additional properties and sub-designs are required to investigate the behavior of vehicles under control.

Earlier Development in Numerical Control

The history of modern numerical control dates to July, 1949, at the Massachusetts Institute of Technology [6], where an initial research project was carried out under the sponsorship of Parsons Corporation of Traverse City,

Michigan, and the United States Air Force. The two phases of this project consisted of an engineering study aimed toward the development of a system applicable to machine tools for controlling the position of shafts in accordance with the output of a computing machine. Since then the areas in which numerical control have been put to use are increasing. The most important element for any numerically controlled machine tool is the control unit, which is essentially an information-handling device. The control unit accepts information from the input medium, reads it, stores it, interprets it, and generates electrical command pulses which, when acted upon, cause movement of an operational device. The number of command pulses generated determines the displacement of this movement, and the frequency of these command pulses determines the rate of the movement.

A Statement of the Problem

In this study of the vehicular control system, the simple control theory is used to design a linear feedback system which regulates the position and velocity of every vehicle moving in the same guideway lane. The main purpose is to investigate the static and dynamic errors of the system which generates its error signal by counting positively clock pulses and negatively wayside markers. The forward-counting pulse train of the clock is compared to the backward-counting pulse train which is generated within the vehicle as it crosses a pattern of markers embedded in the guideway. The two pulse trains are passed through a bidirectional counter which in turn feeds to the controller as shown in Figure 2. Depending on the error signal in the counter, the controller will cause the vehicle to accelerate or decelerate. Inputs considered are the marker spacings and disturbing forces.

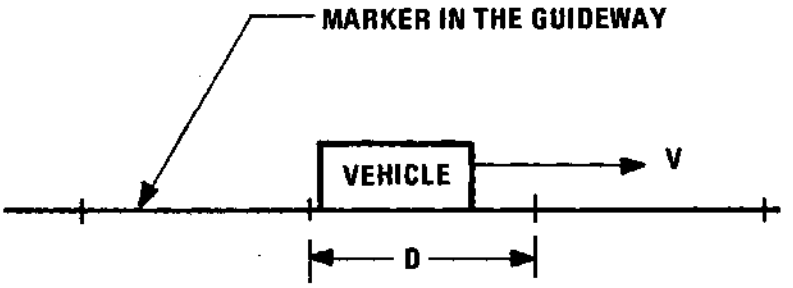

Figure 1. A Vehicle Moving Along the Guideway Lane.

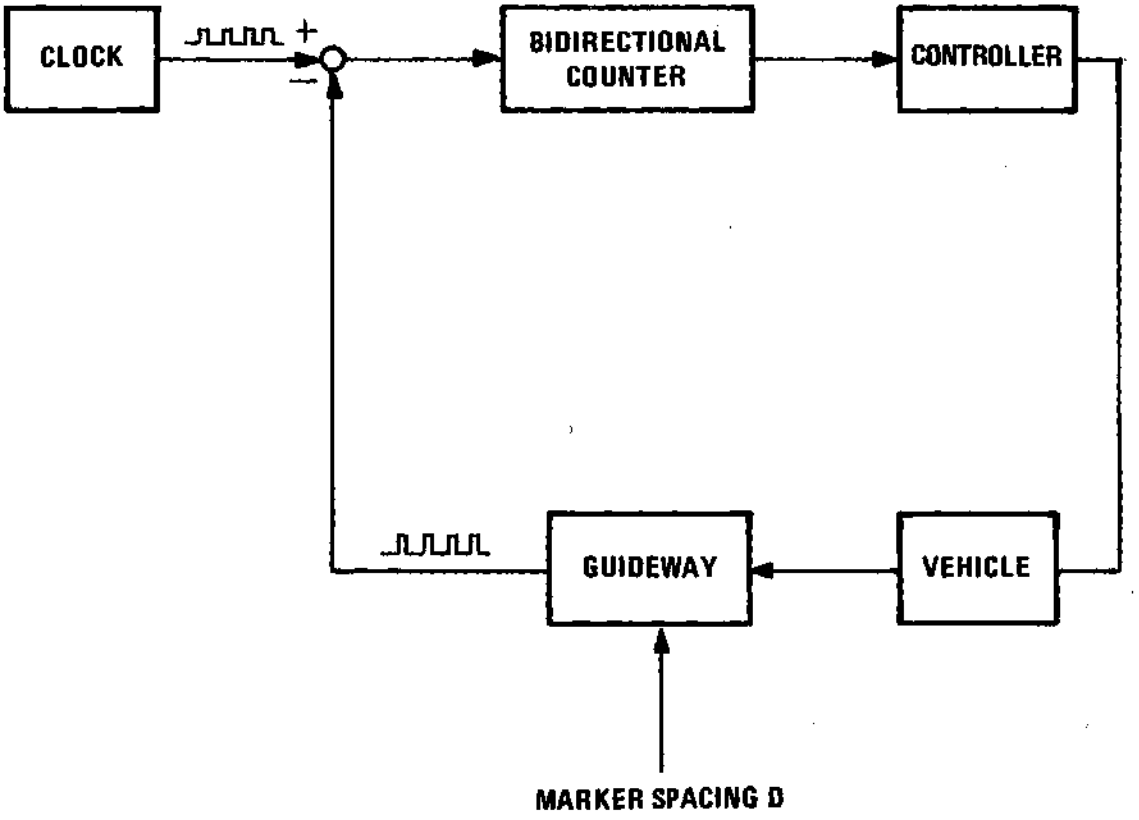

Figure 2. Block Diagram Describing the Physical System.

For step inputs, the error characteristics of the system will be developed.

In Chapter II, the mathematical model is formulated and various parameters of the system are defined. The non-linear equation governing the motion of the vehicle is linearized. The whole system also is normalized for the sake of simplicity in investigation. In Chapter III, the available theory is applied to the solution of the problem. In Chapter IV, the non-linear system is simulated on an analog computer and the results are compared to predict the range of applicability and accuracy of the linear model.

CHAPTER II

FORMULATION OF THE PROBLEM

Mathematical Modelling

Consider a vehicle moving with a velocity V at any time t. The forces acting on the vehicle consist of the force required to accelerate or decelerate the vehicle and the true drag force due to the air opposing the vehicle. Since the wind drag force is proportional to the first power of the air density and the projected area of the vehicle and to the second power of the relative approached velocity of the vehicle, therefore [3]

$$F_W(t) = \frac{c\sigma A V^2}{2g}$$

Assuming that the velocity deviation at steady state is small, then the nonlinear drag force can be linearized to a function of the velocity of the vehicle only. Hence

$$F_W(t) = cV(t)$$

Using this assumption the motion of the vehicle is described by the Newton's law of motion as

$$F(t) - cV(t) = m\dot{V}(t)$$

or

$$mV(t) + c\dot{V}(t) = F(t) \qquad (1)$$

As the vehicle runs over the patterns of the markers located on the roadbed it produces pulses. Therefore the pulse train created by the vehicle at time t is

$$P_V(t) = \frac{V(t)}{D} \tag{2}$$

These pulses are fed back to compare with the reference clock pulses and the counter will count the numbers of the difference in pulses at time t. Hence

$$P_E(t) = P_R(t) - P_V(t) \tag{3}$$

$$E = \int_{t_1}^{t_2} P_E(t)\, dt \tag{4}$$

The controller utilizes the difference of these pulses to actuate the dynamic control force which is

$$F_c(t) = K\int_{t_1}^{t_2} P_E(t)dt \tag{5}$$

The disturbing force is any force, besides the dynamic control force, which has an influence in accelerating or decelerating the moving vehicle such as the slope of the road which the vehicle climbs up. Combining these two forces, the net force applied to the vehicle is

$$F(t) = F_c(t) + F_d(t) \tag{6}$$

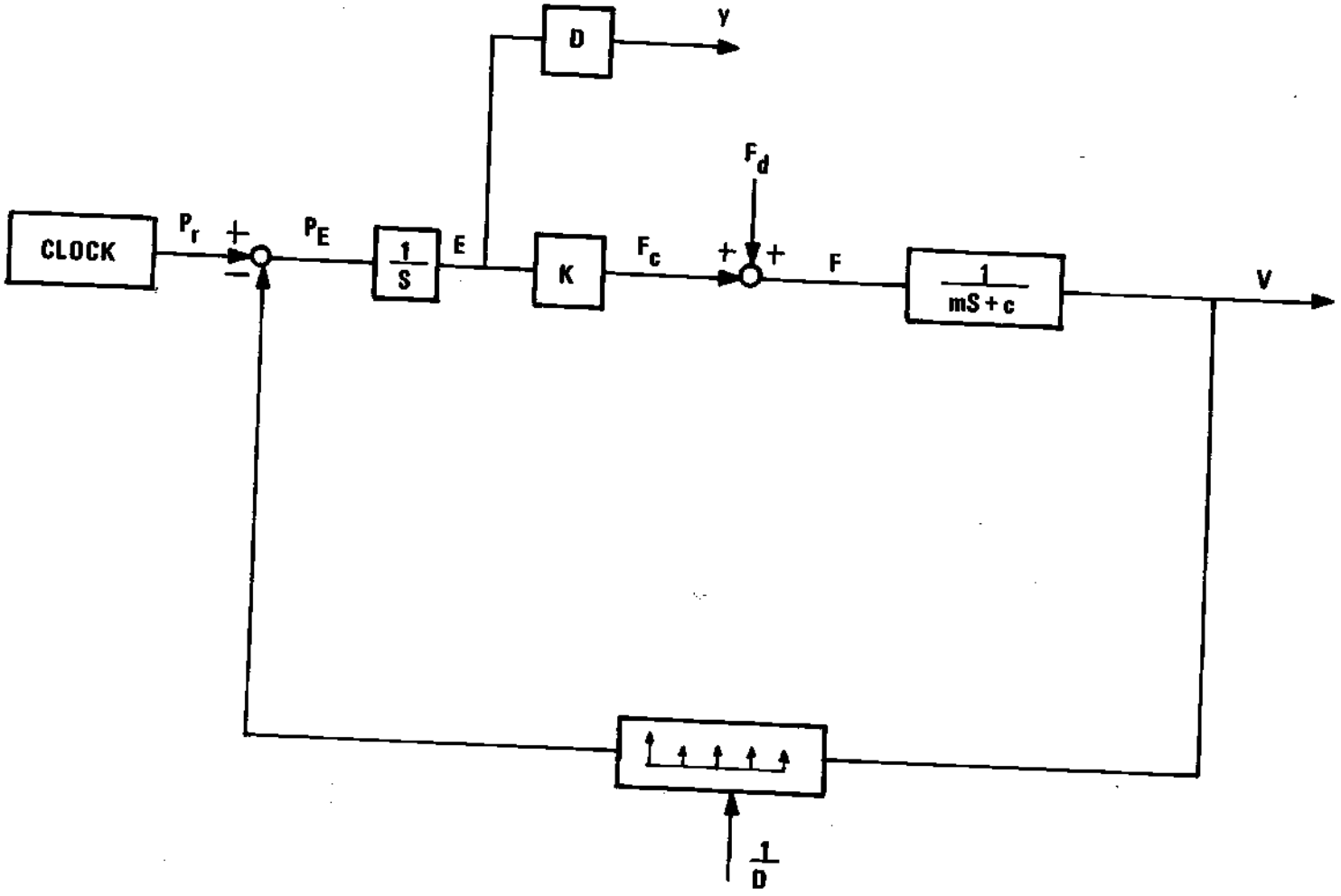

Figure 3. Actual System Block Diagram.

Applying Laplace transformation to the equations (1) to (6), the resulting actual system block diagram can be drawn as shown in Figure 3.

System Normalization

The time constant [4] of the system is

$$T = \frac{m}{c}$$

Let the normalized time of the system be

$$t = T\tau$$

Then the equation (1) can be written as

$$\dot{V}(t) + \frac{1}{T} V(t) = \frac{F(t)}{m}$$

or

$$\frac{\dot{V}(t)}{T} + \frac{V(t)}{T} = \frac{F(t)}{m}$$

Let

$$v(t) = TV(t)$$

Then the above equation becomes

$$\frac{\dot{v}(t)}{T^2} + \frac{v(t)}{T^2} = \frac{F(t)}{m} \qquad (7)$$

Define the normalized net applied force as

$$f(t) = \frac{T^2}{m} F(t)$$

the equation (7) is

$$\overset{+}{v}(t) + v(t) = f(t)$$

By normalizing the parameters of the system in this way, the other parameters can be transformed as shown in Table 1. The normalized system block diagram is shown in Figure 4.

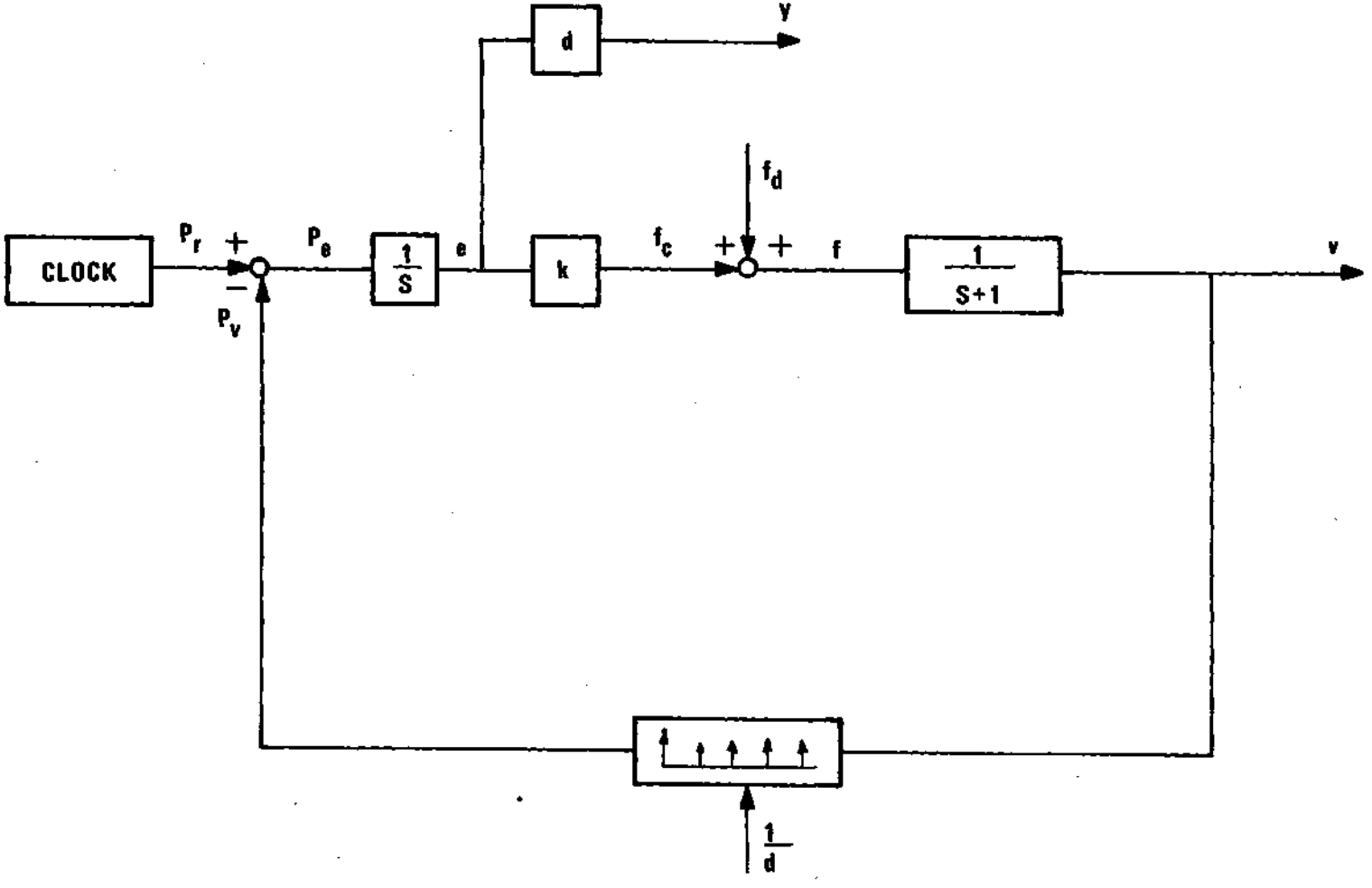

Figure 4. Normalized System Block Diagram.

Table 1. Conversion Factors from the Actual System to the Normalized System

Actual System Parameters	Multiplied by Parameters	Normalized System Parameters
D	1	d
$F(t)$	$\frac{T^2}{m}$	$f(t)$
$F_c(t)$	$\frac{T^2}{m}$	$f_c(t)$
$F_d(t)$	$\frac{T^2}{m}$	$f_d(t)$
K	$\frac{T^2}{m}$	k
E	T	e
$P_R(t)$	T	$P_r(t)$
$P_V(t)$	T	$P_v(t)$
$P_E(t)$	T	$P_e(t)$
$V(t)$	T	$v(t)$
$Y(t)$	1	$y(t)$
$Y_{max}(t)$	1	$y_{max}(t)$

Table 1 (Continued). Conversion Factors from the Actual System to the Normalized System

Actual System Parameters	Multiplied by Parameters	Normalized System Parameters
$Y_{SS}(t)$	1	$y_{SS}(t)$
Ω_d	T	ω_d
Ω_n	T	ω_n
t	$\frac{1}{T}$	τ

Note: $T = \frac{m}{c}$ = second

CHAPTER III

ANALYTICAL SOLUTION OF THE PROBLEM

Solution Due to the Disturbance

Since the important parameters of the system are f(t), d and k, therefore the characteristics of the system related to these parameters will be derived.

Consider the system subjected to the disturbing force as a step input, the system block diagram of Figure 4 will be as shown in Figure 5. From Figure 5 we have

$$\frac{y(S)}{f_d} = - \frac{d}{dS(S+1) + k}$$

$$\ddot{y}(t) + \dot{y}(t) + \frac{k}{d} y(t) = - f_d \tag{8}$$

Define

$$\omega_n^2 = \frac{k}{d}$$

$$\xi = \frac{1}{2} \sqrt{\frac{d}{k}}$$

$$\omega_d = \omega_n \sqrt{1 - \xi^2}$$

$$\phi = \cos^{-1} \xi$$

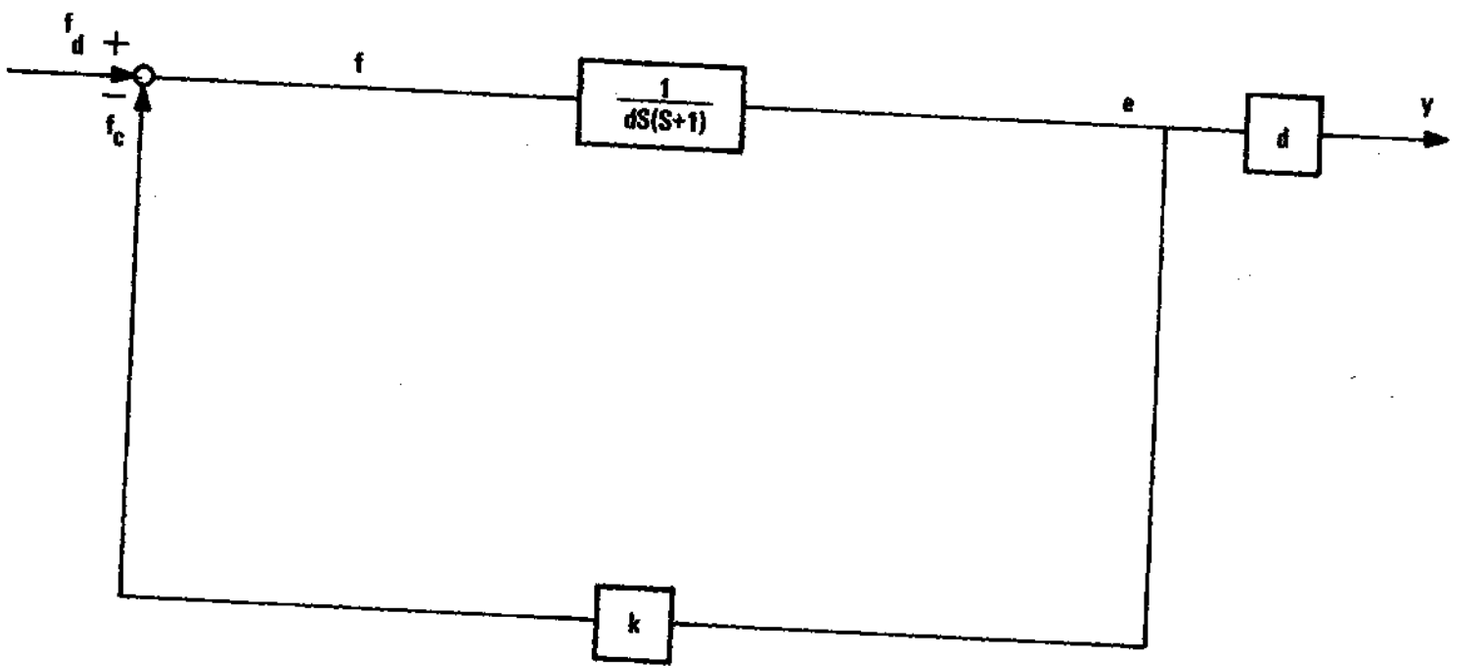

Figure 5. The System Block Diagram for Use in Investigating the Disturbing Force.

then the equation (8) becomes

$$\ddot{y}(t) + 2\xi\,\omega_n \dot{y}(t) + \omega_n^2\, y(t) = -f_d$$

Taking the Laplace transformation with zero initial conditions

$$y(S) = \frac{-f_d}{S(S^2+2\xi\,\omega_n S+\omega_n^2)}$$

or

$$y(S) = \frac{\omega_n^2 X}{S(S^2+2\xi\,\omega_n S+\omega_n^2)}$$

where

$$X = -\frac{d}{k}\, f_d$$

Taking the inverse Laplace transformation, then [5]

$$y(t) = X\left[1 - \frac{\omega_n}{\omega_d}\, e^{-\xi\omega_n t}\, \sin(\omega_d t+\phi)\right] \qquad (9)$$

From equation (9) the steady state error is

$$y_{SS} = -\frac{d}{k}\, f_d$$

It is seen that by increasing k or decreasing d, the unwanted system error can be made smaller. However the smaller value of $\frac{d}{k}$ will reduce the damping ratio. This means that a more oscillatory response will result. Therefore the

compromise in choosing the system gain and the distance between the markers must be made.

In solving for the maximum error we differentiate the equation (9) with respect to time and then equate it to zero. Hence

$$\dot{y}(t) = \frac{X\,\omega_n}{\omega_d}\left[\xi\,\omega_n e^{-\xi\,\omega_n t}\sin(\omega_d t+\phi) - \omega_d e^{-\xi\omega_n t}\cos(\omega_d t+\phi)\right]$$

or $\xi\,\omega_n \sin(\omega_d t+\phi) - \omega_d \cos(\omega_d t+\phi) = 0$

$$t = \frac{1}{\omega_d}\left[\tan^{-1}\left(\frac{\omega_d}{\xi\,\omega_n}\right) - \phi\right] \qquad (10)$$

But the response equation (9), which is composed of an exponential decay term and a sine term, is derived by the Laplace transformation technique with all initial conditions at zero. Therefore the time in equation (10) corresponds to the first zero-valued derivative. This means that we obtain the minimum value of the error, i.e.

$$t = 0$$

Therefore

$$\tan^{-1}\left(\frac{\omega_d}{\xi\,\omega_n}\right) = \phi$$

for all values of ω_d, ξ, ω_n and ϕ.

Also the maximum error will occur at the first decaying period of the response equation. Hence

$$t_{max} = \frac{\pi}{\omega_d} \tag{11}$$

The numerical values of various parameter groups are calculated by the digital computer and the result is tabulated in Table 2. Note that the parameter groups are dimensionless. Also the result is plotted as shown in Figure 6.

Table 2. Computer Values of the Normalized System Due to f_d

ξ	k/d	ω_n	ω_d	t_{max}	Y_{SS}/f_d	Y_{max}/f_d	Per Cent Overshoot
0.20	6.250	2.500	2.449	1.282	-0.160	-0.244	52.50
0.25	4.000	2.000	1.936	1.621	-0.250	-0.361	44.40
0.30	2.778	1.667	1.590	1.975	-0.360	-0.494	37.20
0.40	1.562	1.250	1.145	2.741	-0.640	-0.802	25.30
0.50	1.000	1.000	0.866	3.626	-1.000	-1.163	16.30
0.60	0.694	0.833	0.667	4.710	-1.440	-1.576	9.45
0.70	0.510	0.714	0.510	6.156	-1.960	-2.050	4.59
0.80	0.390	0.625	0.375	8.373	-2.560	-2.599	1.52
0.90	0.308	0.555	0.242	12.966	-3.240	-3.245	0.15
1.00	0.250	0.500			-4.000		
1.10	0.206	0.454			-4.840		
1.20	0.173	0.417			-5.760		

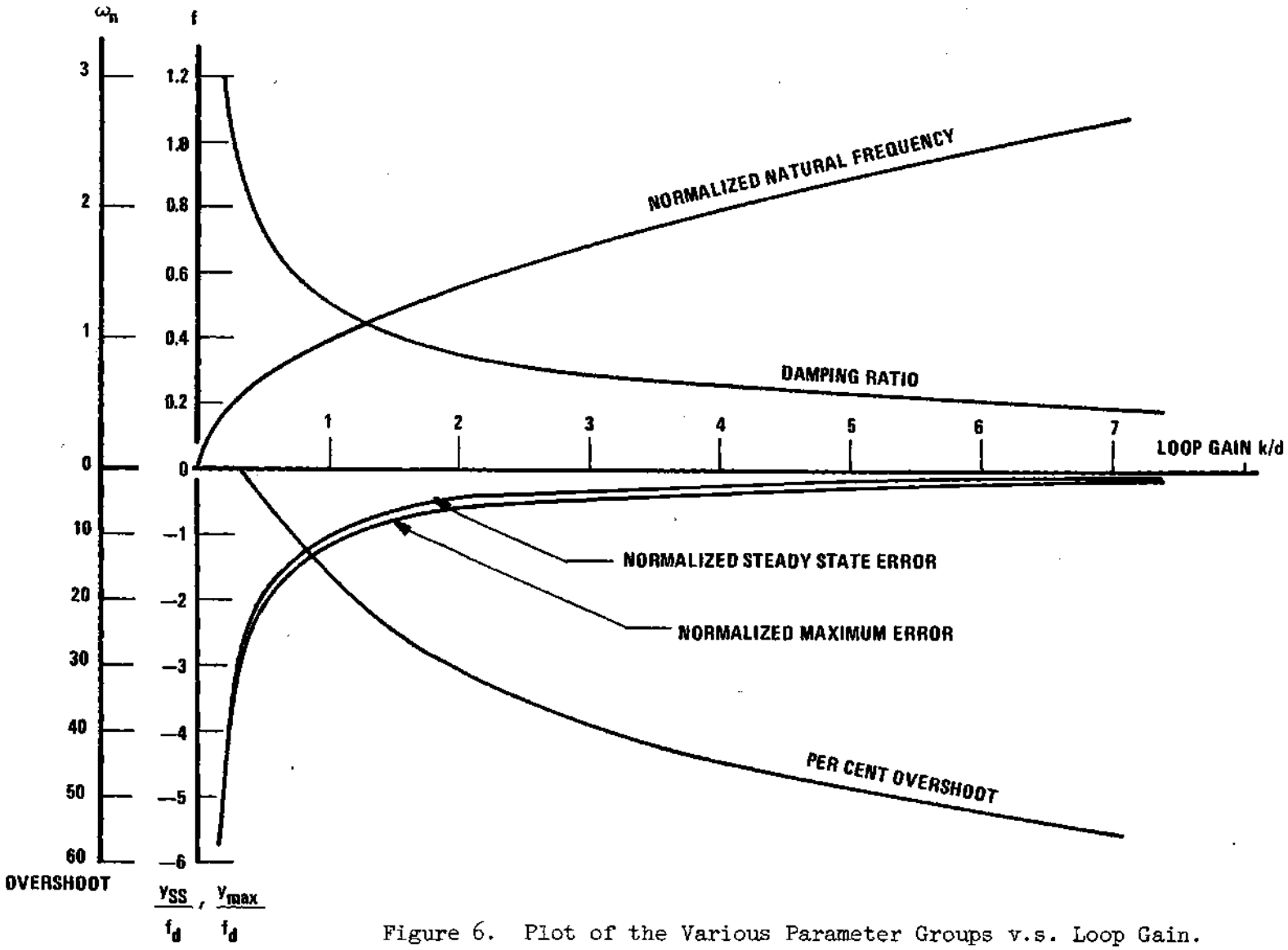

Figure 6. Plot of the Various Parameter Groups v.s. Loop Gain.

Solution Due to the Clock Pulses

In investigating this situation, the disturbing input is assumed to be zero. Therefore the system block diagram of Figure 4 becomes as shown in Figure 7. Hence

$$\frac{y(S)}{P_r} = \frac{d^2(S+1)}{dS(S+1)+k}$$

or

$$\ddot{y}(t) + \dot{y}(t) + \frac{k}{d}\, y(t) = d(\dot{P}_r + P_r) \tag{12}$$

To find the response, assume a step clock pulse input. With the system initially in some equilibrium condition, the equation (12) becomes

$$(S^2 + S + \frac{k}{d})\, y(S) = d\left[s\left(\frac{P_r}{S}\right) - P_r + \left(\frac{P_r}{S}\right) \right]$$

$$(S^2 + S + \frac{k}{d})\, y(S) = \frac{dP_r}{S} \tag{13}$$

Define

$$\omega_n^2 = \frac{k}{d}$$

$$\xi = \frac{1}{2}\sqrt{\frac{d}{k}}$$

$$\omega_d = \omega_n \sqrt{1 - \xi^2}$$

$$\phi = \cos^{-1}\xi$$

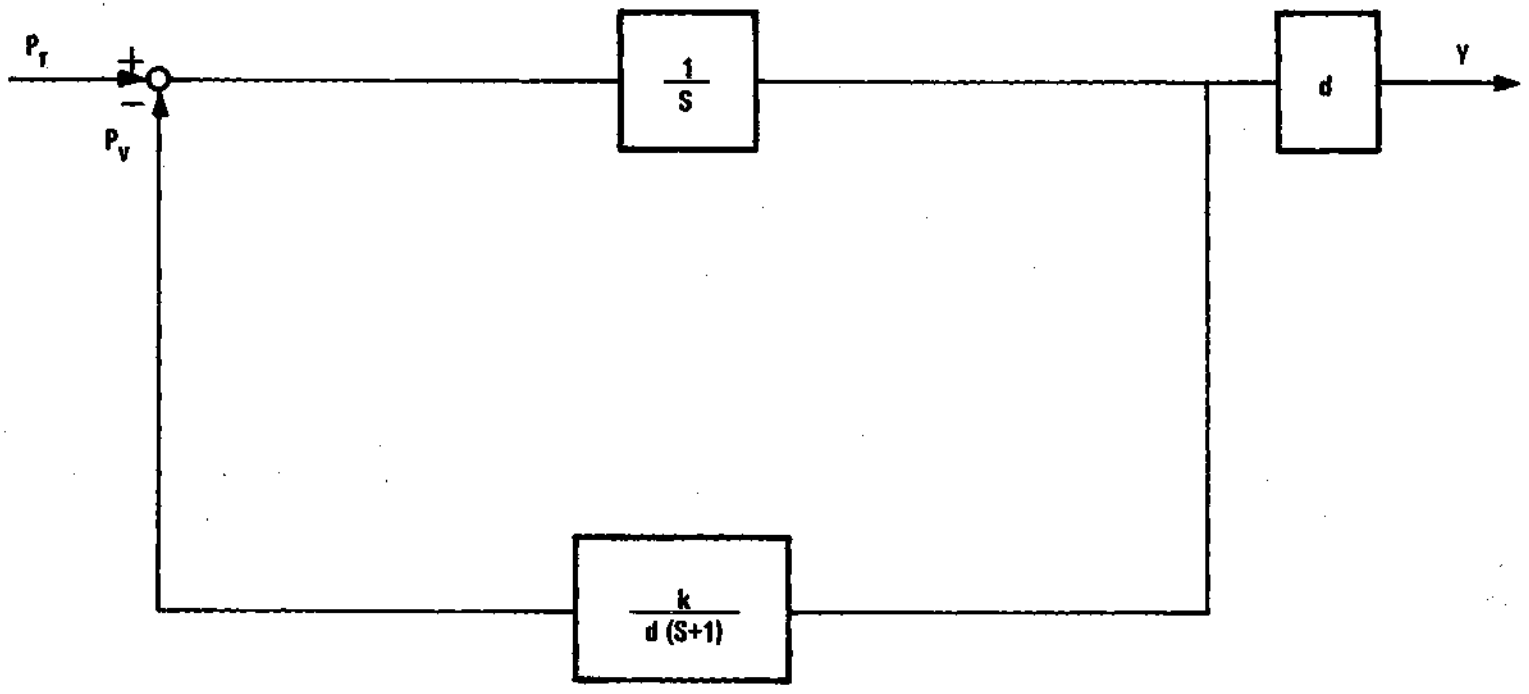

Figure 7. The System Block Diagram for Use in Investigating the Clock Pulses and Marker Spacing.

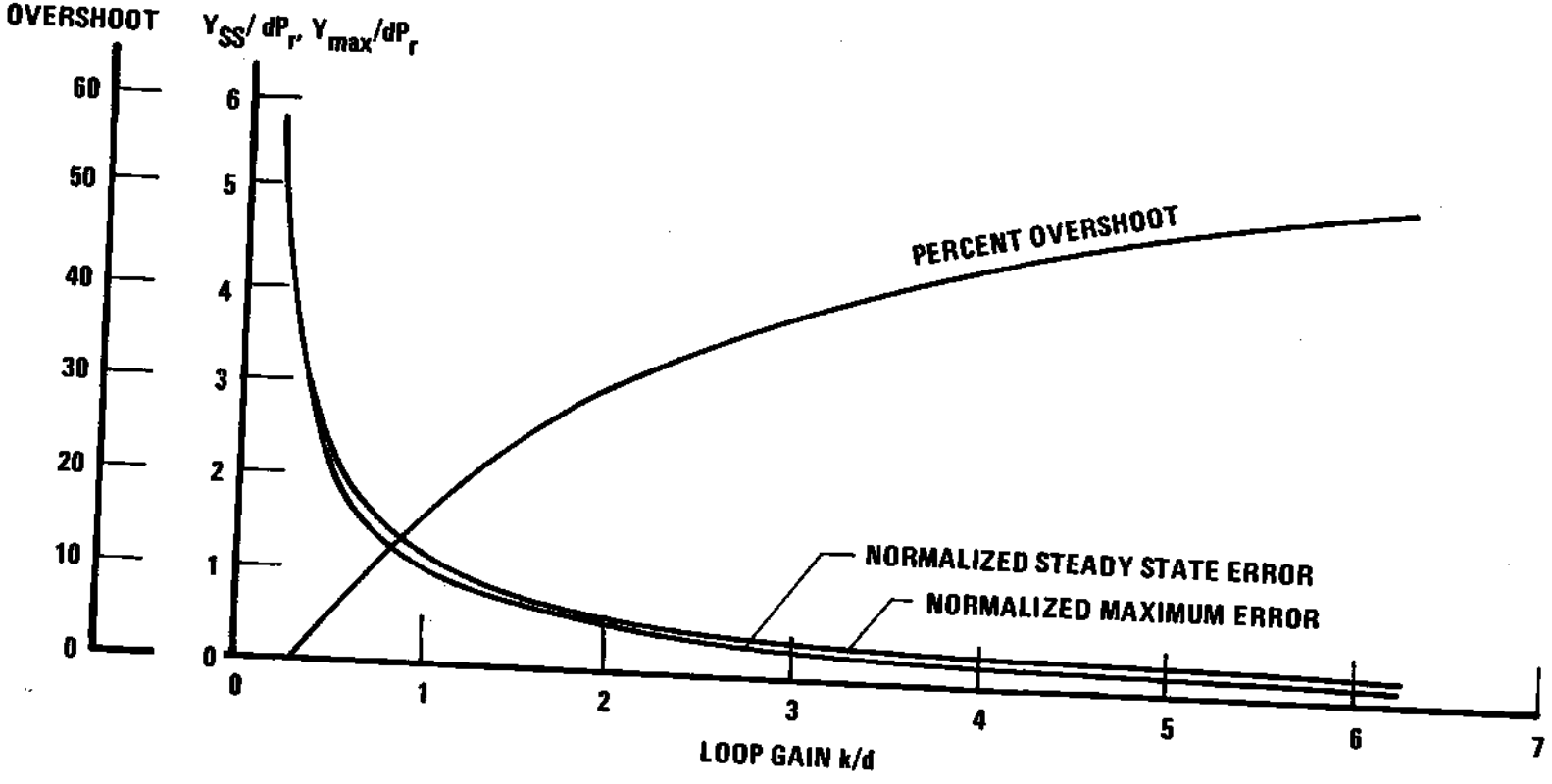

Figure 8. Plot of Parameter Groups v.s. Loop Gain.

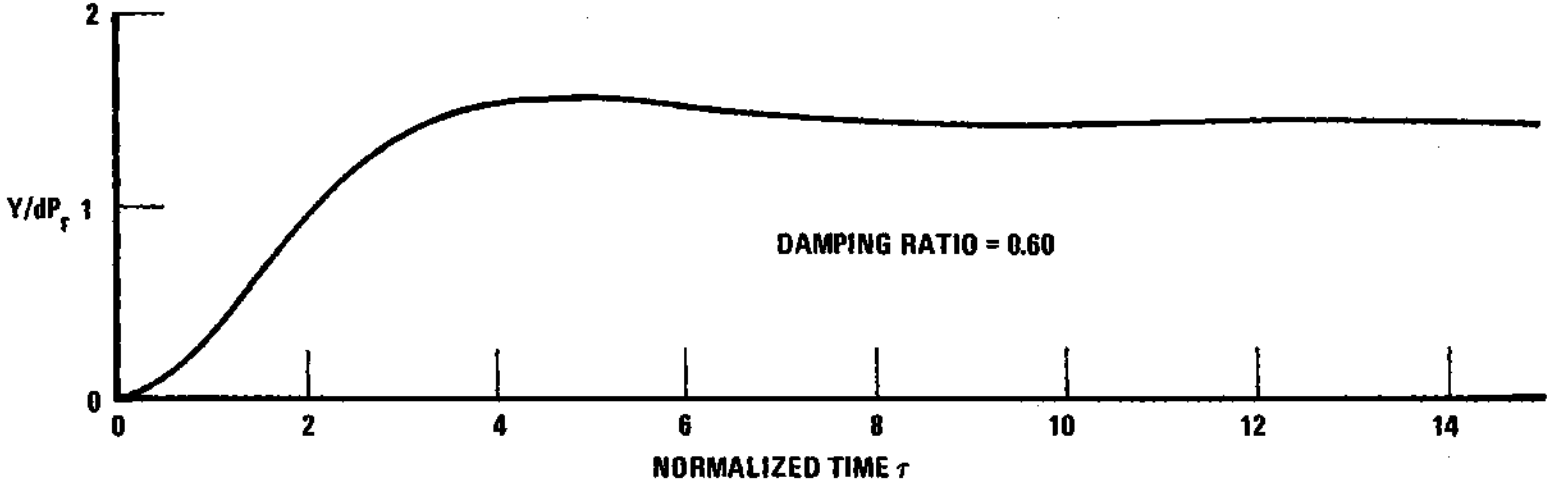

Figure 9. Plot of Analytic Results Showing the Distance Error v.s. Time.

then the equation (13) can be arranged as

$$y(S) = \frac{dP_r}{S(S^2+2\xi\omega_n S+\omega_n^2)}$$

It is seen that this equation is analog to the one before. Therefore the solution is

$$y(t) = \frac{d^2P_r}{k}\left[1 - \frac{\omega_n}{\omega_d} e^{-\xi\omega_n t} \sin(\omega_d t + \phi)\right] \qquad (14)$$

Also the time at which the maximum error occurs is

$$t_{max} = \frac{\pi}{\omega_d} \qquad (15)$$

The numerical values of parameter groups are tabulated in Table 3 and the result is plotted as shown in Figure 8.

Table 4 shows the analytic results at the typical damping ratio of 0.60 and the resulting curve is as shown in Figure 9. Small overshoots indicate that the linearized model is a good control system.

Solution Due to a Step Change in Marker Spacing

Consider a step change in the marker spacing from d_1 to d_2. The situation at this instant is shown in Figure 10. Before making a step change of the marker spacing the vehicle is assumed to be in the equilibrium condition, that is its

Table 3. Computed Values of the Normalized System Due to Clock Pulses

ξ	y_{SS}/dP_r	y_{max}/dP_r	Per Cent Overshoot
0.20	0.160	0.244	52.50
0.25	0.250	0.361	44.40
0.30	0.360	0.494	37.20
0.40	0.640	0.802	25.30
0.50	1.000	1.163	16.30
0.60	1.440	1.576	9.45
0.70	1.960	2.050	4.59
0.80	2.560	2.599	1.52
0.90	3.240	3.245	0.15
1.00	4.000	4.000	0
1.10	4.840		
1.20	5.760		

Table 4. Typical Values of the Distance Error at $\xi = 0.60$

Normalized Time τ	Normalized Distance Error y/dP_r
0.50	0.105
1.00	0.348
1.50	0.643
2.00	0.929
2.50	1.171
3.00	1.355
3.50	1.477
4.00	1.546
4.50	1.574
5.00	1.573
5.50	1.554
6.00	1.528
6.50	1.500
7.00	1.475
7.50	1.455
8.00	1.441
8.50	1.432
9.00	1.428
9.50	1.427

Table 4 (Continued). Typical Values of the Distance Error at $\xi = 0.60$

Normalized Time τ	Normalized Distance Error y/dP_r
10.00	1.428
10.50	1.431
11.00	1.433
11.50	1.436
12.00	1.438
12.50	1.439
13.00	1.440
13.50	1.441
14.00	1.441
14.50	1.441
15.00	1.441
15.50	1.440
16.00	1.440

condition is the steady state error. Therefore the lagging pulses are

$$e = \frac{d_1 P_r}{k}$$

When making a step change in the marker spacing the distance error will

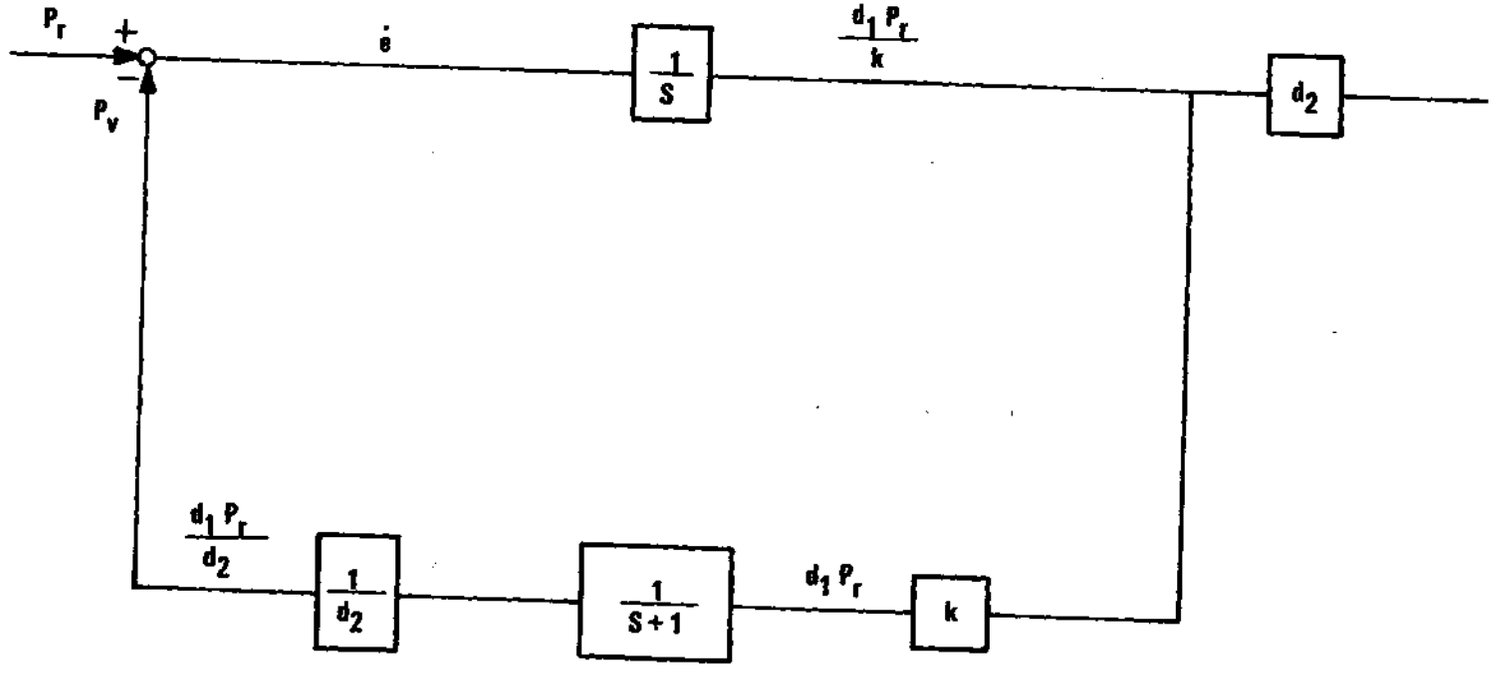

Figure 10. The System Block Diagram for Use in Investigating a Step Change of the Marker Spacing.

jump to

$$y = \frac{d_1 d_2 P_r}{k}$$

and the lagging pulses as seen from Figure 10 is

$$\dot{e} = P_r(1 - \frac{d_1}{d_2})$$

Also

$$\dot{y} = P_r d_2(1 - \frac{d_1}{d_2})$$

$$\xi = \xi_1 \sqrt{\frac{d_2}{d_1}}$$

where ξ_1 is the damping ratio before making a step change in marker spacing. Hence the initial conditions are

$$y(0) = \frac{d_1 d_2 P_r}{k}$$

$$\dot{y}(0) = P_r d_2(1 - \frac{d_1}{d_2})$$

Again the differential equation describing the system is

$$\ddot{y}(t) + 2\xi\omega_n \dot{y}(t) + \omega_n^2 y(t) = d_2 P_r \qquad (16)$$

and the characteristic equation is

$$\ddot{y}(t) + 2\xi\omega_n\dot{y}(t) + \omega_n^2 y(t) = 0$$

Roots of the above characteristic equation are

$$r = \frac{-2\xi\omega_n \pm \sqrt{(2\xi\omega_n)^2 - 4\omega_n^2}}{2}$$

$$= -\xi\omega_n \pm \omega_n\sqrt{\xi^2 - 1}$$

For an underdamped system $\xi < 1$

Hence

$$r = -\xi\omega_n \pm j\omega_d$$

Therefore the complementary solution is

$$y_c(t) = e^{-\xi\omega_n t}(c_1 \sin\omega_d t + c_2 \cos\omega_d t)$$

Let the particular solution be y_P

Then from equation (16)

$$\omega_n^2 y_P = d_2 P_r$$

$$y_P = \frac{d_2 P_r}{\omega_n^2}$$

$$= \frac{d_2^2 P_r}{k}$$

Therefore the general solution is

$$y(t) = \frac{d_2^2 P_r}{k} + e^{-\xi \omega_n t} (c_1 \sin \omega_d t + c_2 \cos \omega_d t) \qquad (17)$$

c_2 can be found by imposing the first initial condition as

$$\frac{d_1 d_2 P_r}{k} = \frac{d_2^2 P_r}{k} + c_2$$

$$c_2 = -\frac{d_2^2 P_r}{k} \left(1 - \frac{d_1}{d_2}\right)$$

c_1 can be evaluated by differentiating the equation (17) as

$$\dot{y}(t) = \omega_d e^{-\xi \omega_n t} (c_1 \cos \omega_d t - c_2 \sin \omega_d t) - \xi \omega_n e^{-\xi \omega_n t} (c_1 \sin \omega_d t + c_2 \cos \omega_d t)$$

$$P_r d_2 \left(1 - \frac{d_1}{d_2}\right) = \omega_d c_1 - \xi \omega_n c_2$$

$$c_1 = \frac{1}{\omega_d} \left[P_r d_2 \left(1 - \frac{d_1}{d_2}\right) + \xi \omega_n c_2 \right]$$

Substitute c_2 into the above c_1, hence

$$c_1 = \frac{d_2^2 P_r}{k} \frac{\omega_n}{\omega_d} \left(1 - \frac{d_1}{d_2}\right) (\omega_n - \xi)$$

Therefore the equation (17) becomes

$$y(t) = \frac{d_2^2 P_r}{k} \left[1 - e^{-\xi \omega_n t} \frac{\omega_n}{\omega_d} \left(1 - \frac{d_1}{d_2}\right) \left\{ (\xi - \omega_n) \sin \omega_d t + \frac{\omega_d}{\omega_n} \cos \omega_d t \right\} \right] \qquad (18)$$

But

$$\frac{\omega_d}{\omega_n} = \sqrt{1 - \xi^2}$$

$$= \sin \phi$$

Hence the above equation is arranged to

$$y(t) = \frac{d_2^2 P_r}{k} \left[1 - e^{-\xi\omega_n t} \frac{\omega_n}{\omega_d} \left(1 - \frac{d_1}{d_2}\right) \left\{ \sin(\omega_d t + \phi) - \omega_n \sin \omega_d t \right\} \right] \qquad (19)$$

To find the time for the extremum, the equation (18) is differentiated and equated to zero.

$$-\omega_d \left[(\xi - \omega_n) \cos \omega_d t - \frac{\omega_d}{\omega_n} \sin \omega_d t \right] + \xi\omega_n \left[(\xi - \omega_n) \sin \omega_d t + \frac{\omega_d}{\omega_n} \cos \omega_d t \right] = 0$$

Rearranging

$$\left[\xi \omega_n^2 (\xi - \omega_n) + \omega_d^2 \right] \sin \omega_d t = -\omega_d \omega_n^2 \cos \omega_d t$$

$$\tan \omega_d t = \frac{\omega_d \omega_n^2}{\xi \omega_n^2 (\omega_n - \xi) - \omega_d^2}$$

Since the value of tangent is positive in the first and third quadrant, therefore the time at which the extremum occurs is

$$t = \frac{1}{\omega_d} \left[\tan^{-1} \left(\frac{\omega_d \omega_n^2}{\xi \omega_n^2 (\omega_n - \xi) - \omega_d^2} \right) + n\pi \right] \qquad (20)$$

where

$$n = 1, 2, 3, 4, \ldots .$$

By computing various values on the digital computer it is found out that for n = 1, the maximum overshoot governs the system for $d_1 > d_2$, and the maximum undershoot does for $d_1 < d_2$.

For n = 2, the reverse is true. But the overshoot and undershoot are less than the former ones. Since fluctuation of the distance error from the steady state error will effect the separation between the vehicles at the moment a step change in marker spacings is made, therefore the values of the maximum and minimum errors at n = 1 will be considered here. The numerical values of parameter groups are tabulated in Table 5. The resulting curves are similar to Figure 8 therefore they will not be shown here.

Table 5. Computed Values of the Normalized System Due to Step Changes in Marking Spacing

	$\frac{d_1}{d_2} = 0.70$			$\frac{d_1}{d_2} = 0.90$			$\frac{d_1}{d_2} = 1.10$			$\frac{d_1}{d_2} = 1.30$		
ξ_1	ξ	$\frac{y_{min}}{d_2 P_r}$	Per cent undershoot	ξ	$\frac{y_{min}}{d_2 P_r}$	Per cent undershoot	ξ	$\frac{y_{max}}{d_2 P_r}$	Per cent overshoot	ξ	$\frac{y_{max}}{d_2 P_r}$	Per cent overshoot
0.200	0.239	0.186	18.534	0.211	0.163	8.200	0.191	0.160	10.113	0.175	0.167	35.788
0.250	0.299	0.320	10.438	0.264	0.264	4.869	0.238	0.241	6.220	0.219	0.235	22.574
0.300	0.358	0.484	5.946	0.316	0.388	2.952	0.286	0.340	3.927	0.263	0.317	14.664
0.400	0.478	0.898	1.840	0.422	0.703	1.083	0.381	0.591	1.596	0.351	0.524	6.397
0.500	0.597	1.422	0.464	0.527	1.107	0.362	0.477	0.915	0.622	0.438	0.790	2.750
0.600	0.717	2.056	0.072	0.632	1.598	0.096	0.572	1.312	0.214	0.526	1.120	1.095
0.700	0.837	2.800	0.003	0.738	2.177	0.016	0.667	1.783	0.057	0.614	1.513	0.374
0.800	0.956	3.657	0.000	0.843	2.844	0.001	0.763	2.327	0.009	0.702	1.971	0.096

CHAPTER IV

SYSTEM SIMULATION

The equation already derived in Chapter II is simulated on an analog computer. The program of the linear system and that of the non-linear one are shown in Figures 11 and 12 respectively. In both cases an integrator is used to represent a real counter. For a linear system the reference clock pulses and the feedback pulse trains generated within the vehicle are simply represented by the voltage sources.

Figure 13 is the simulation result with the vehicle initially at rest. The values of the controller gain, k, are varied from 0.60 to 0.90. It is seen that as the controller gain increased the steady state error decreased but a more oscillatory response and an increase in overshoot resulted. Figure 14 shows that as the marker spacing, d, is increased the steady state error also increased and a less oscillatory response and overshoot are obtained. It is also observed that a small increment in the marker spacing, in this case from 1 to 1.30, results in a large steady state error. The comparison of the response with and without initial velocity is shown in Figure 15. The results indicate that the former gives less overshoot than the latter.

The above results can be explained by considering the analytic solutions obtained in Chapter III as

$$y_{SS} = \frac{d^2 P_r}{k}$$

$$\xi = \frac{1}{2}\sqrt{\frac{d}{k}}$$

$$\omega_n = \sqrt{\frac{k}{d}}$$

It is seen that as the marker spacing increased the steady state error is increased to a factor of d^2 and the damping ratio is also increased while the natural frequency is decreased. The increase in the damping ratio gives a less overshoot response but the decrease in the natural frequency yields a slower response time.

Figure 16 shows the resulting response from the disturbing force alone. The characteristics of the response curve are similar to the former results except that the steady state error is negative for a positive disturbing force. This means that additional force on the vehicle subjected to a positive disturbing force is required. Therefore the combination of the clock pulse and disturbing force inputs will give less steady state error as shown in Figure 17.

In the simulation of the non-linear system the reference clock pulse is one cycle per second. The feedback pulse trains are similar to those of the real system but the counter is still represented by an integrator. Figure 12 shows the complete schematic diagram of the analog computer program of the non-linear system used to simulate on Systron Donner model 10-20. In this simulation the force applied to the vehicle is plotted instead of the distance error because a part of the controller gain, k, exists in the counter itself. The values of damping ratios, controller gains, marker spacings, and potentiometer settings are tabulated in Table 6.

Figures 18 through 20 are the results of simulation of the non-linear system as compared to the linear one at 0.60 damping ratio, but different values of the controller gain and marker spacing. The three compared curves show that the linear response is the average of the non-linear one. It is seen that as the marker spacings and controller gains are increased the pulse amplitudes also increased. This means that the linear system gives less approximation to the non-linear system at higher values of the marker spacing and controller gain. It can be explained by considering the real system that, at a given damping ratio, the displacement of the vehicle is smoother for the smaller marker spacing and applied force than the larger one.

Figures 21 through 23 are the simulation results at 0.80 damping ratio. In this case the overshoot, as known from analytical results in Chapter III, is only 1.52 per cent. Therefore it cannot be observed in the curves. It is seen that between 2.50 to 5 second per normalized time the linear response shows more deviation from the non-linear one than at the lower damping ratio. Because of higher damping ratios the slower speed of response will result. Therefore it can be concluded that the transient response of the linear system at high damping ratios is slower than the non-linear response.

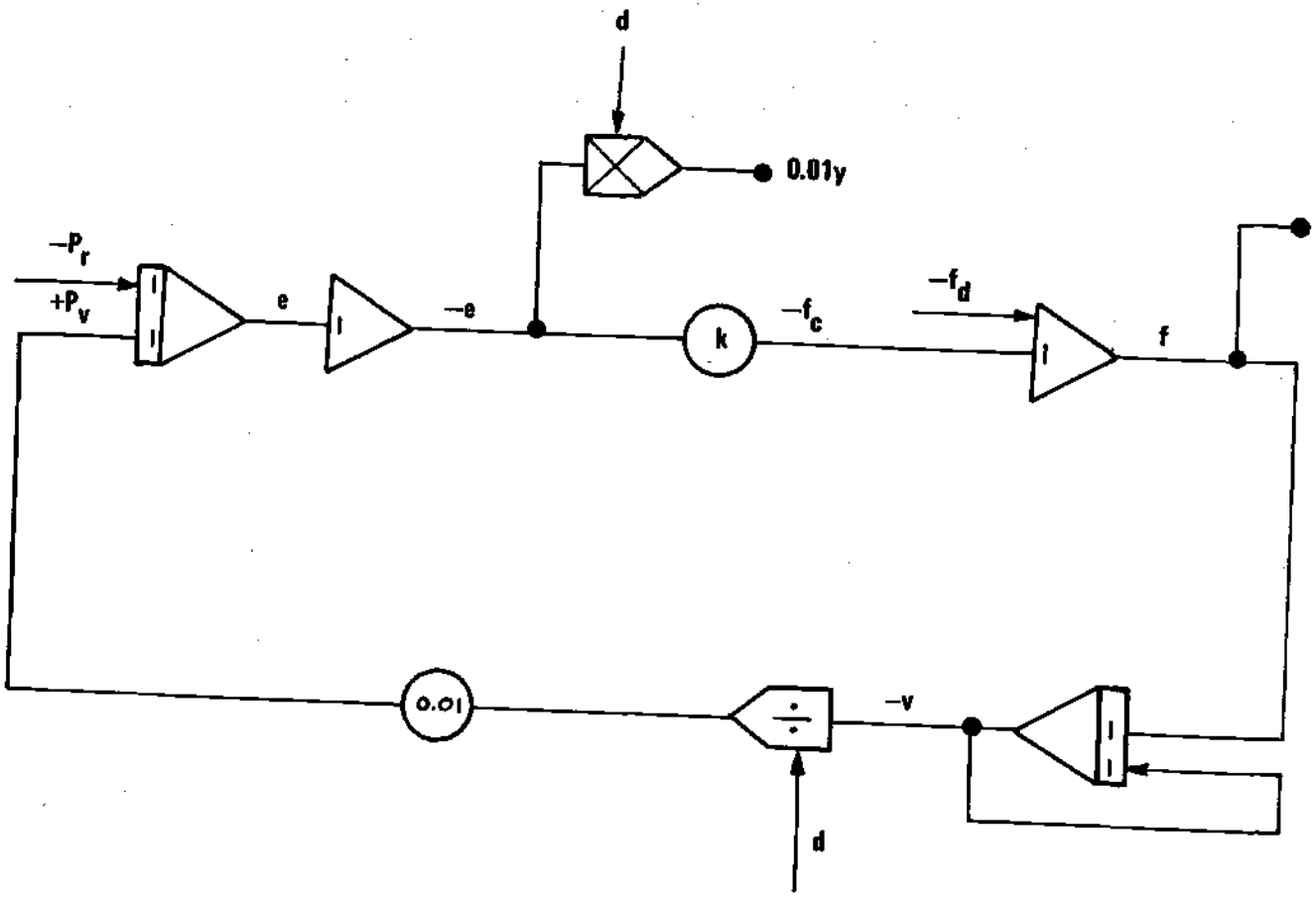

Figure 11. The Schematic Analog Computer Program for the Linear System.

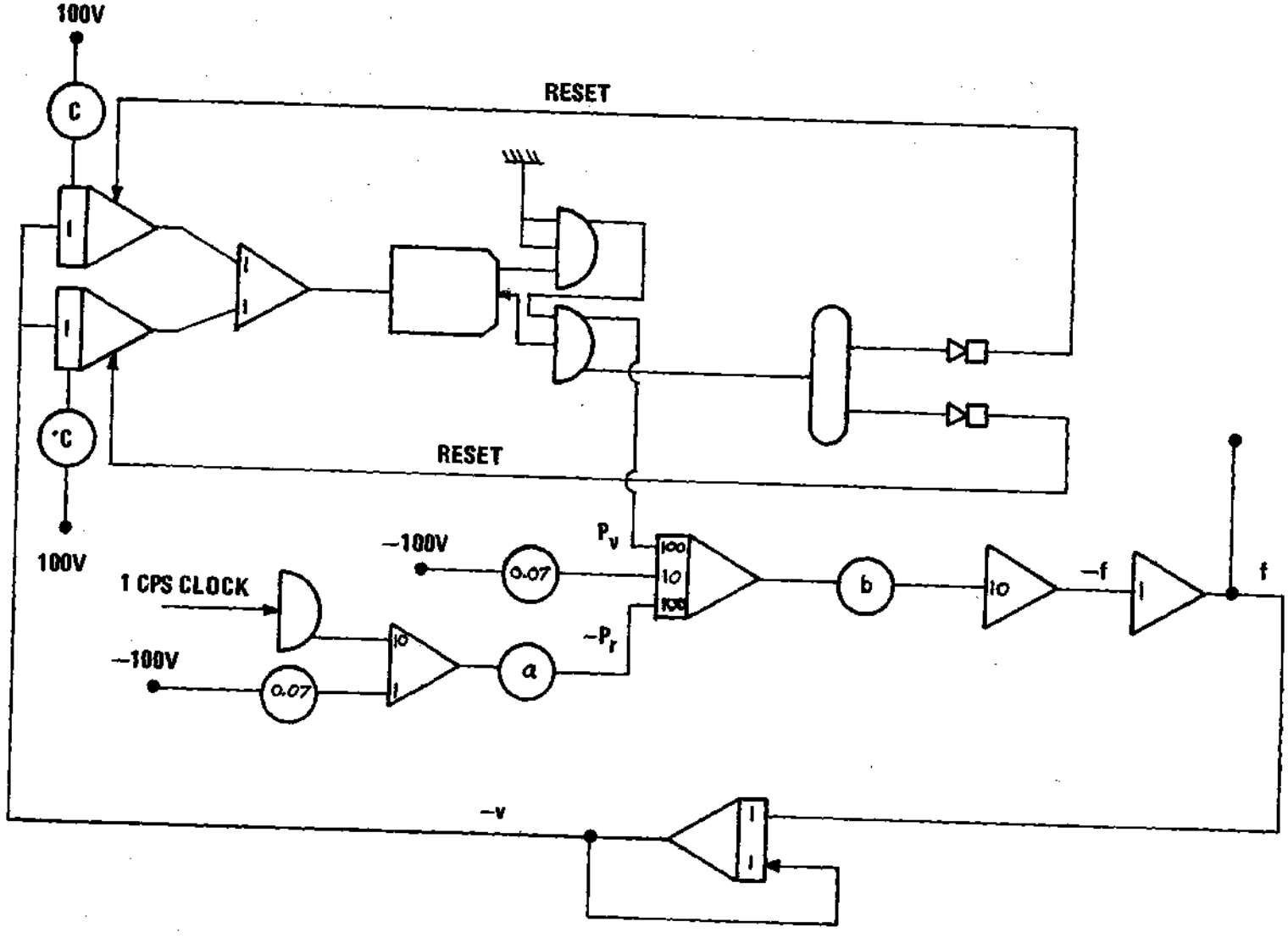

Figure 12. The Schematic Analog Computer Program for the Non-Linear System.

Table 6. The Values of Potentiometer Setting for Figure 12

ξ	k	d	a	b	c
0.60	6.950	10	0.410	0.080	0.050
0.60	10.040	15	0.270	0.180	0.075
0.60	13.900	20	0.220	0.290	0.100
0.80	3.910	10	0.410	0.050	0.050
0.80	5.850	15	0.270	0.110	0.075
0.80	7.810	20	0.220	0.170	0.100

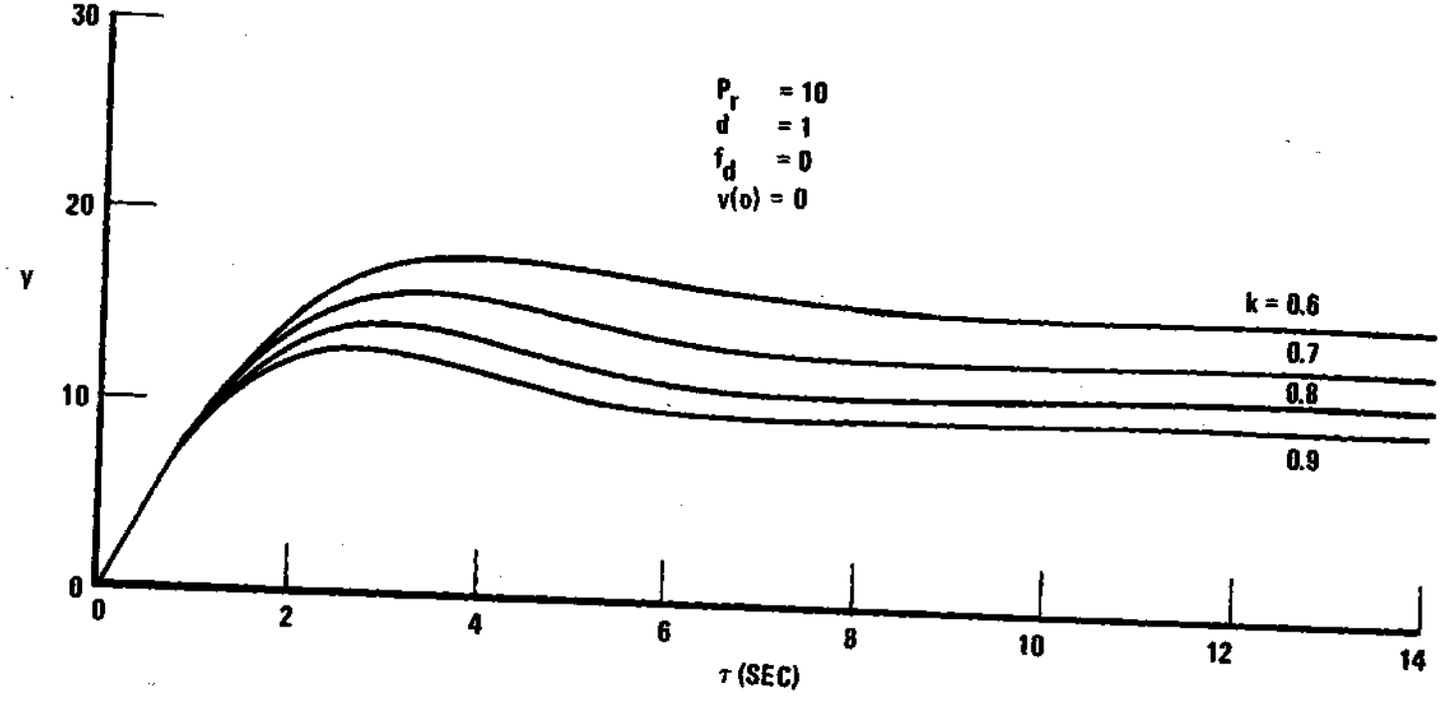

Figure 13. Results from Simulation Showing the Distance Error v.s. Time with I.C. = 0.

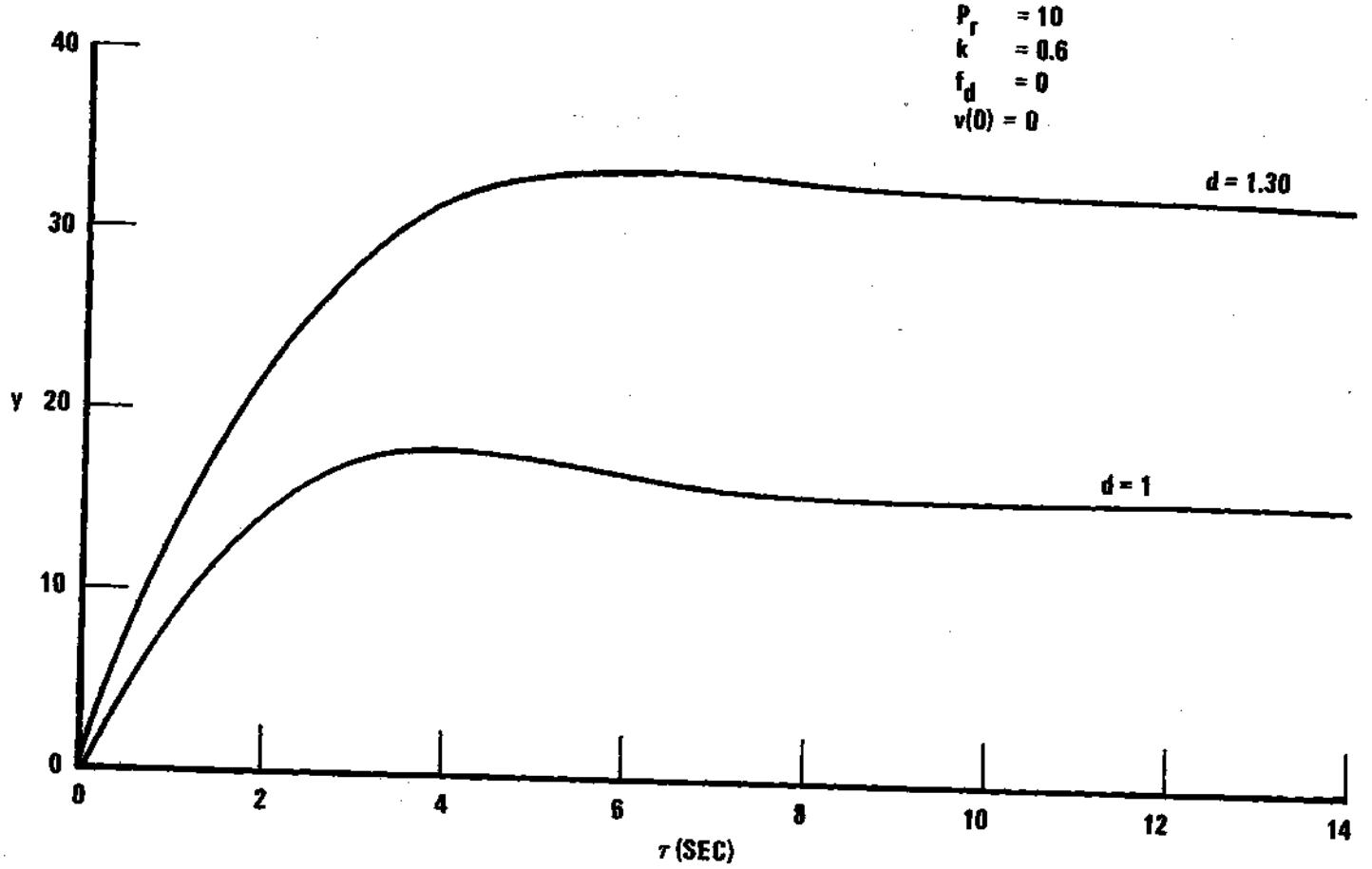

Figure 14. Results from Simulation Showing the Distance Error v.s. Time with Different Wayside Spacing.

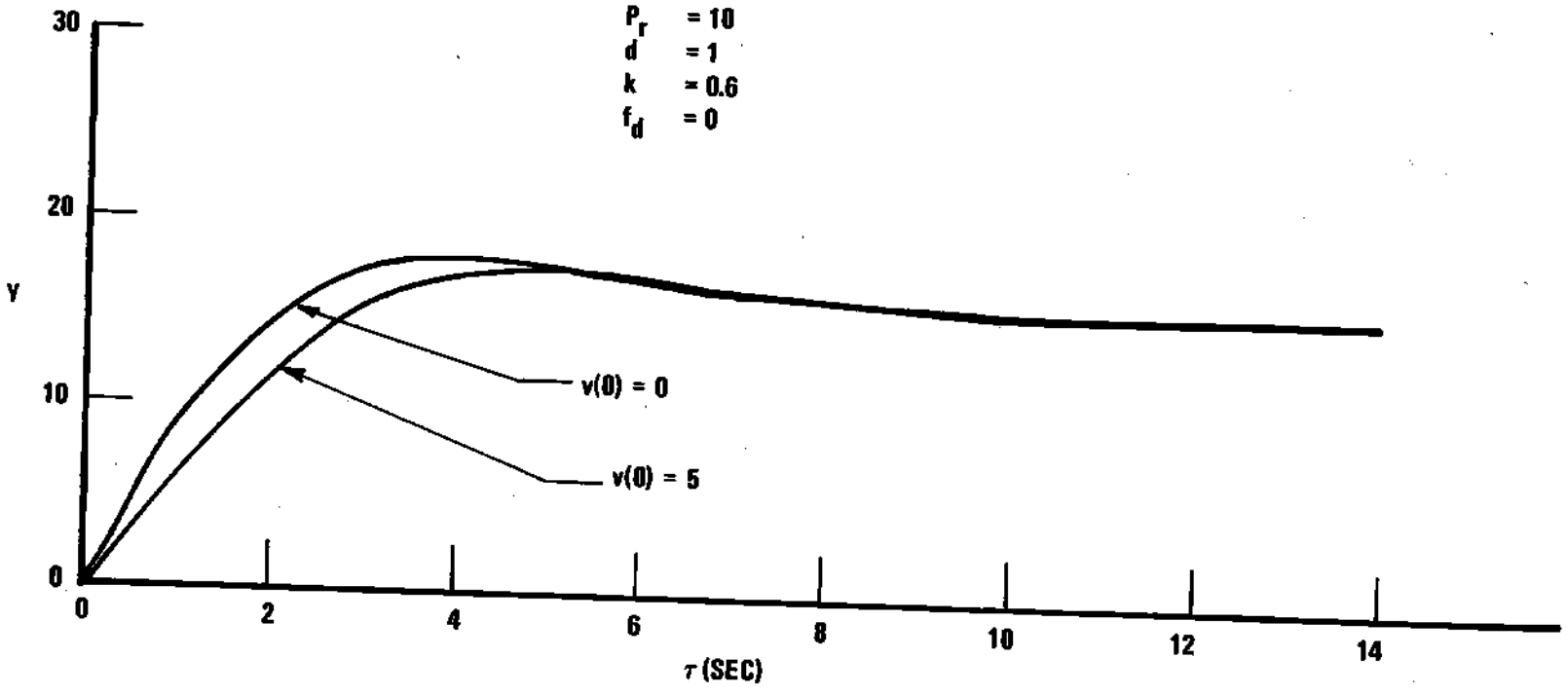

Figure 15. Results from Simulation Showing the Distance Error v.s. Time with Different I.C.

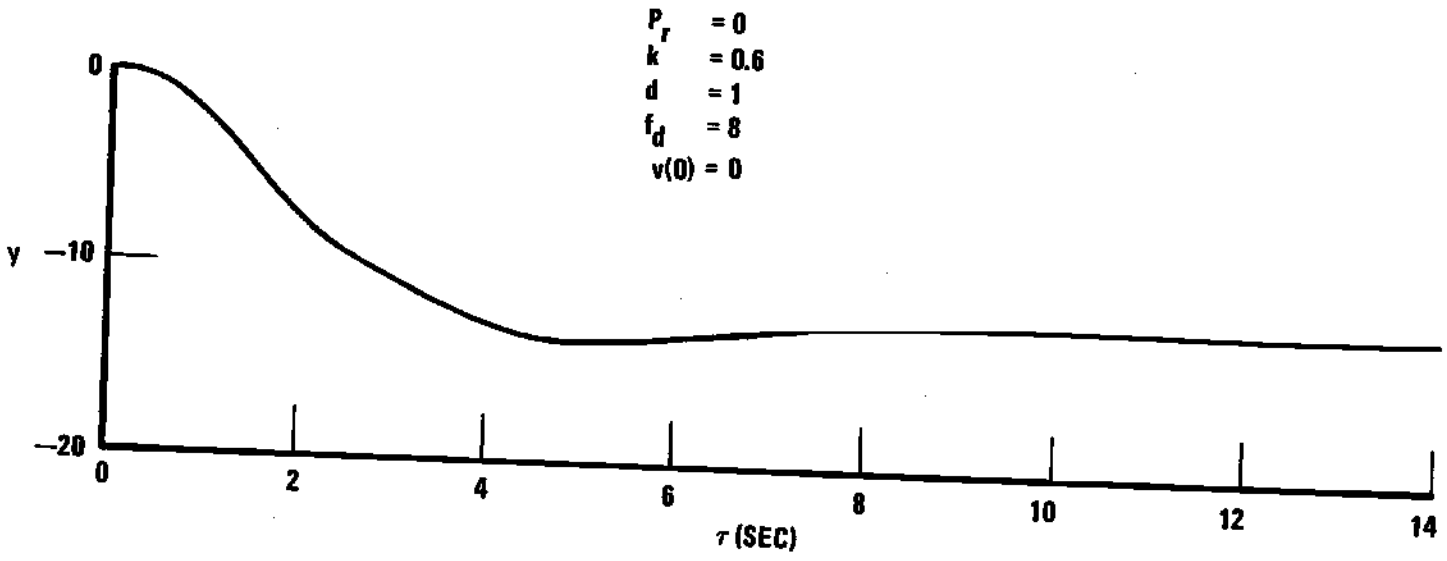

Figure 16. Results from Simulation Showing the Distance Error v.s. Time, Subjected to the Disturbance.

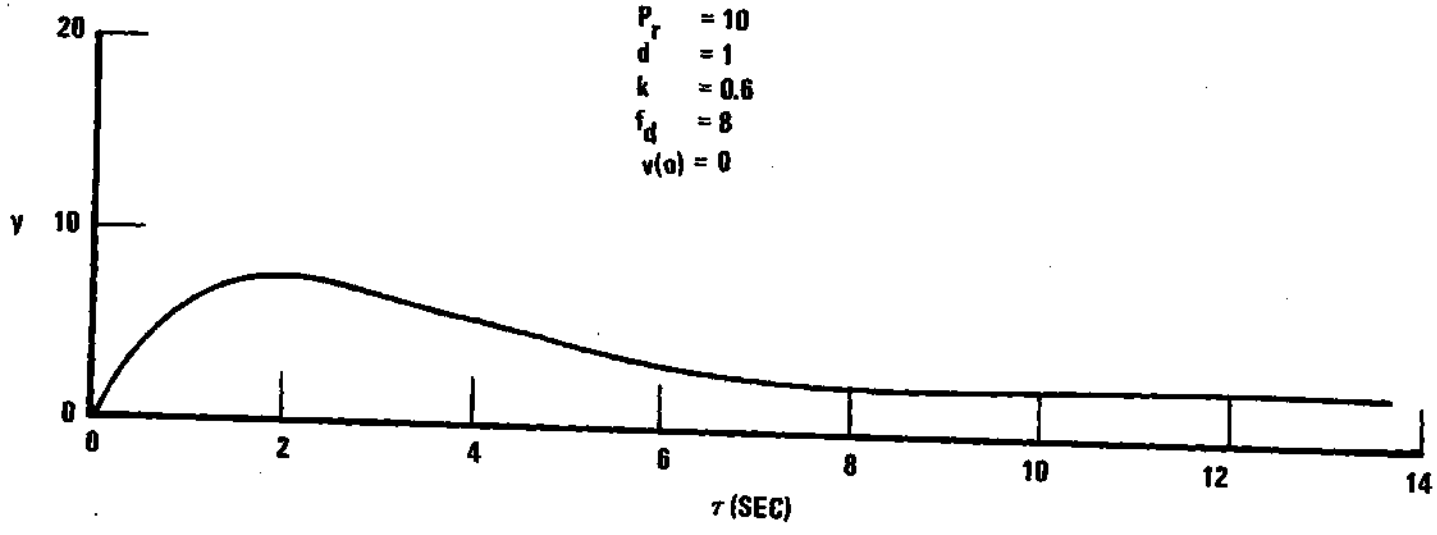

Figure 17. Results from Simulation Showing the Distance Error v.s. Time with Two Inputs and Zero I.C.

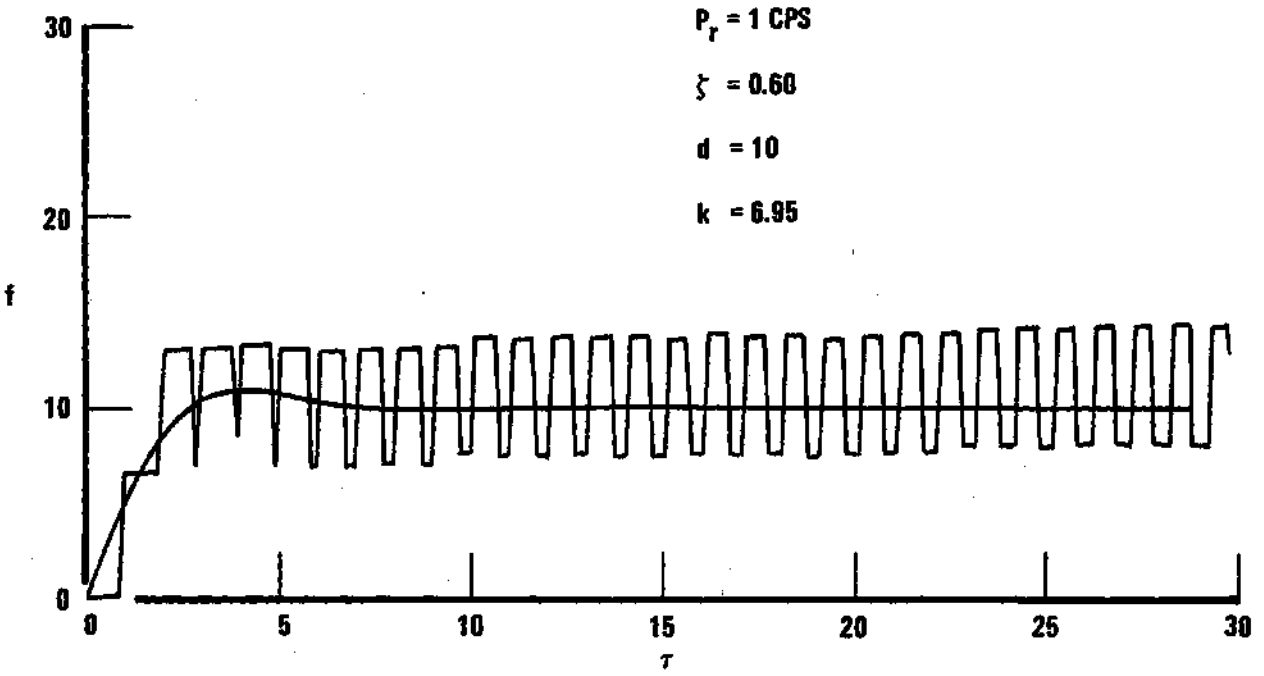

Figure 18. Results from Simulation Showing the Comparison of the Linear and Non-Linear System at 0.60 Damping Ratio.

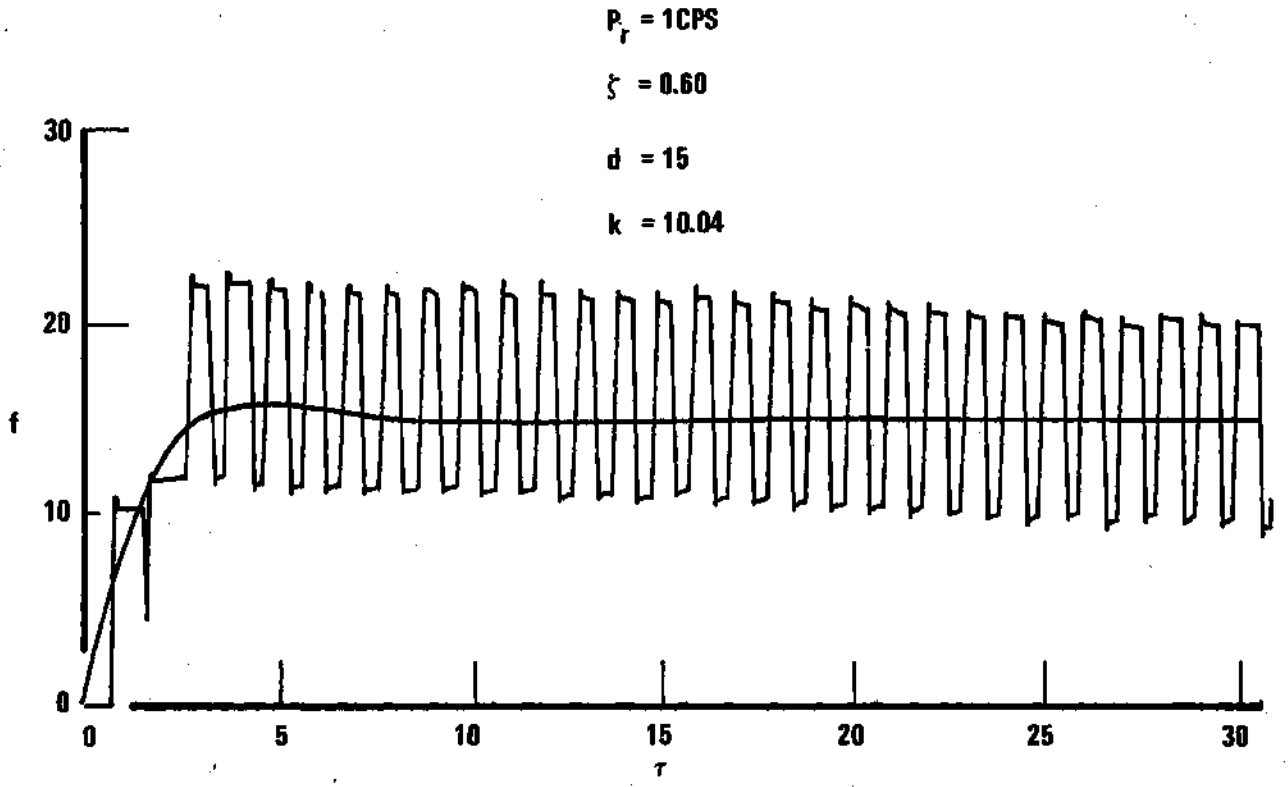

Figure 19. Results from Simulation Showing the Comparison of the Linear and Non-Linear System at 0.60 Damping Ratio.

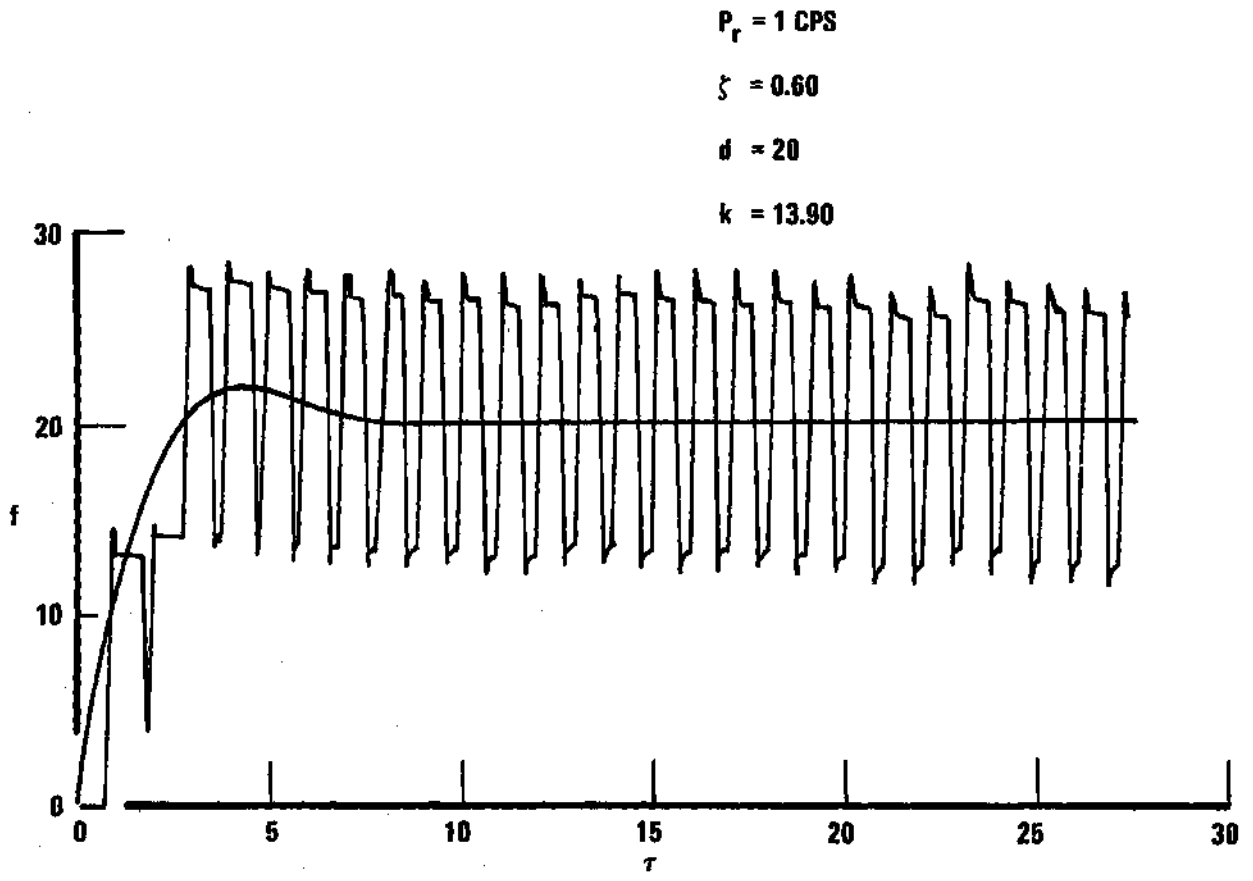

Figure 20. Results from Simulation Showing the Comparison of the Linear and Non-Linear System at 0.60 Damping Ratio.

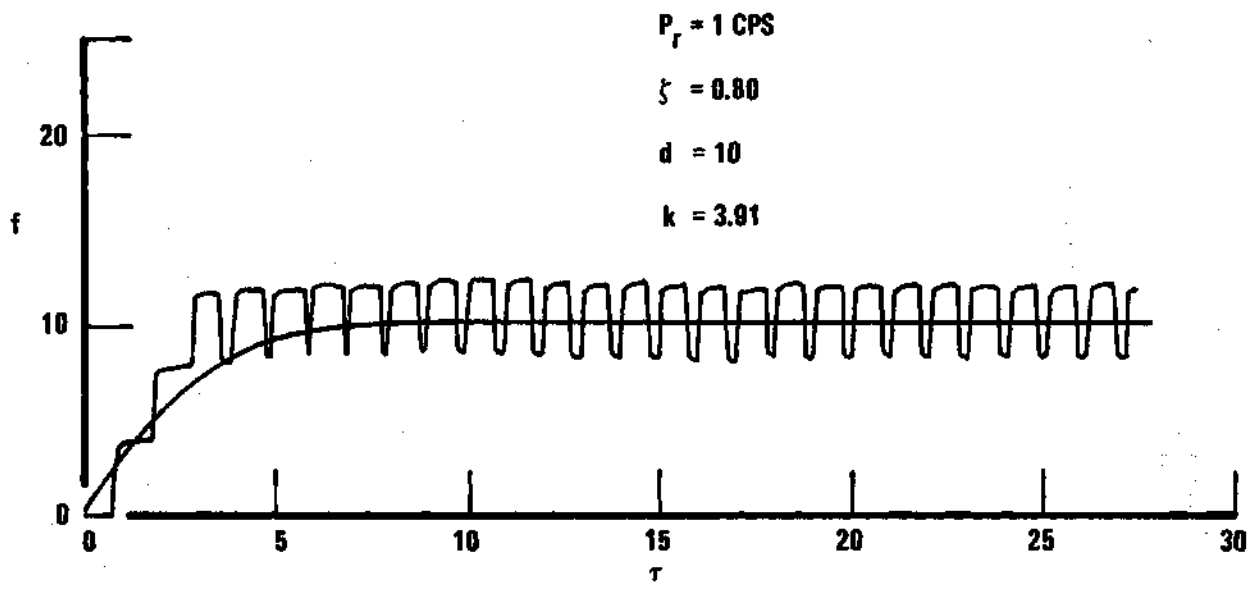

Figure 21. Results from Simulation Showing the Comparison of the Linear and Non-Linear System at 0.80 Damping Ratio.

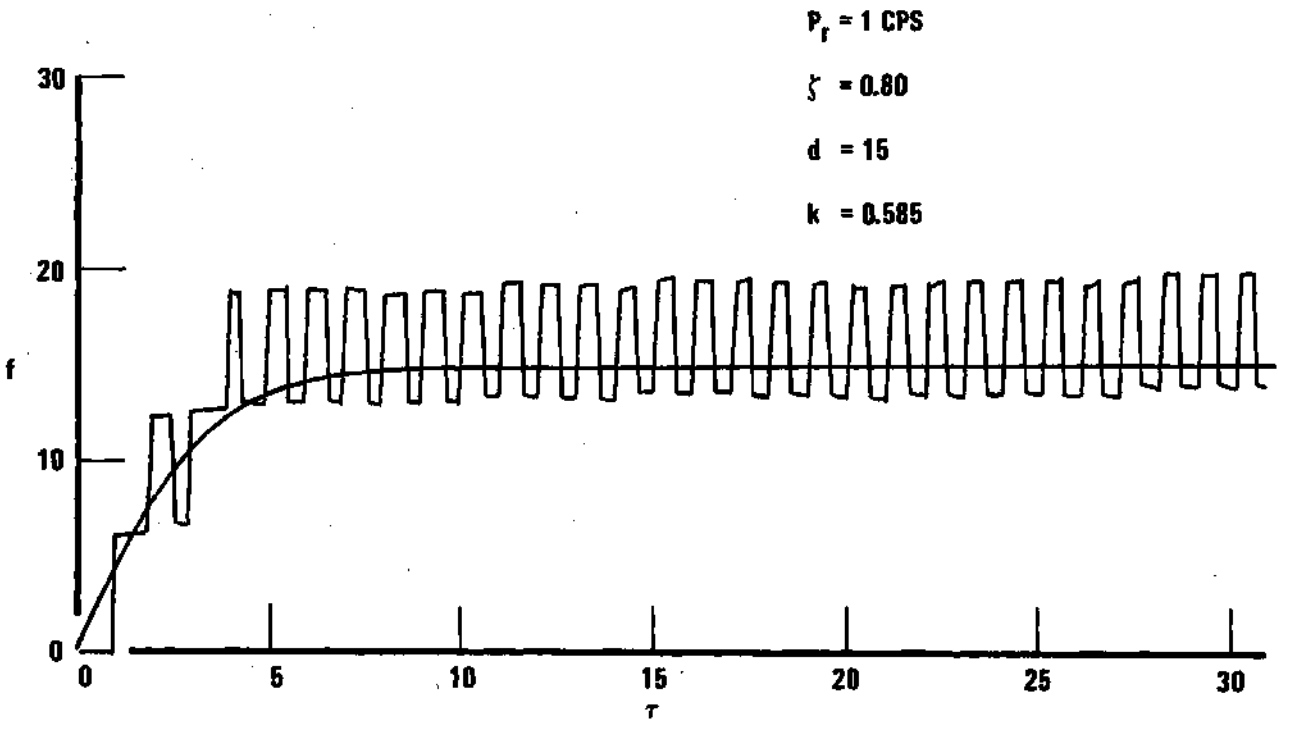

Figure 22. Results from Simulation Showing the Comparison of the Linear and Non-Linear System at 0.80 Damping Ratio.

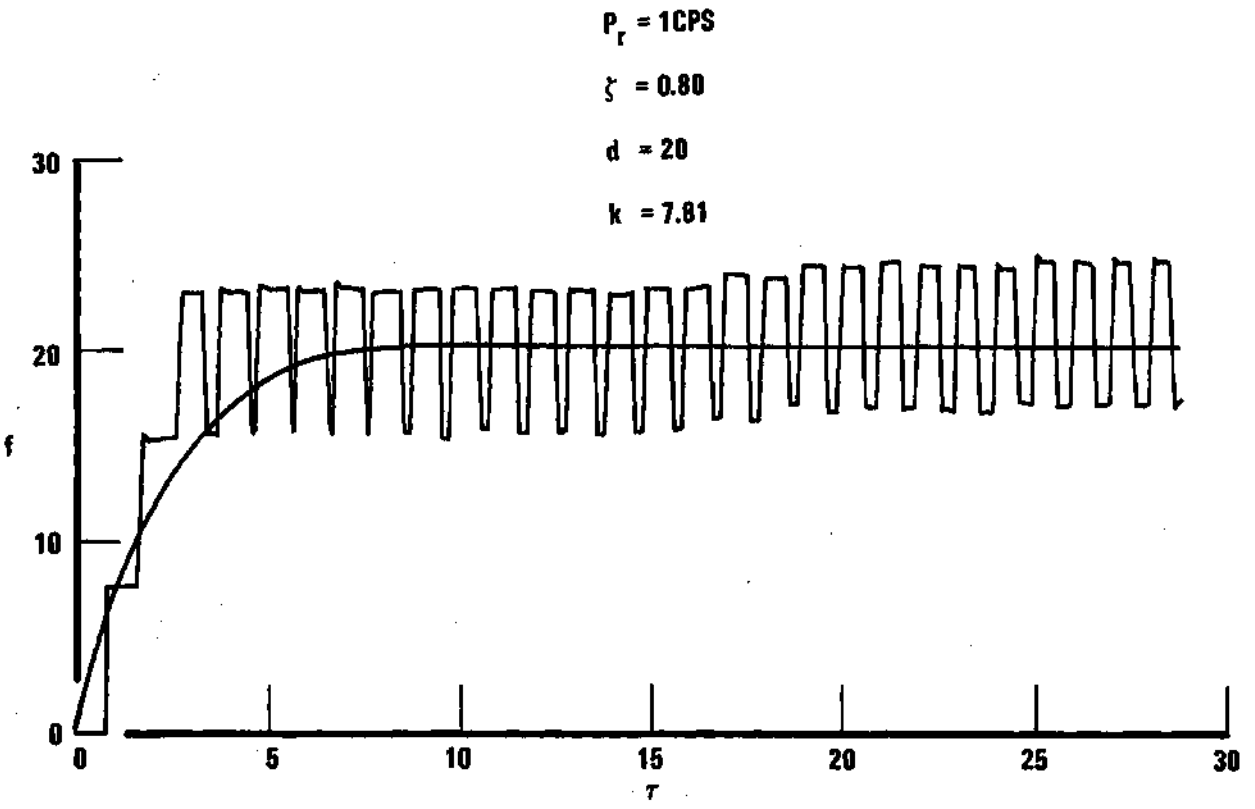

Figure 23. Results from Simulation Showing the Comparison of the Linear and Non-Linear System at 0.80 Damping Ratio.

CHAPTER V

CONCLUSIONS AND DISCUSSION

The general design principles have been presented for a feedback control of the position and velocity of the vehicle. The analytical results of the linear system subjected to the step changes in marker spacing and disturbing force have similar characteristic curves. From Table 2 and 3, it is seen that the steady state error increases with the increase in the damping ratio. It is also found out that the speed of response depends on the ratio of controller gain to marker spacing. The higher values of this ratio will result in the quicker speed of response and the lower steady state error but a more oscillatory response is observed. For the damping ratios ranging between 0.5 to 0.80, the corresponding overshoots are from 16.30 to 1.52 per cent.

For a step change in marker spacing, the response will show undershoots or overshoots depending on whether the step is up or down. Results in Table 5 show that when d_2 is greater than d_1, the damping ratios are increased. This results in larger steady state error and smaller overshoots. When d_2 is less than d_1, the damping ratios are decreased. The overshoots are increased but the steady state error is decreased. Therefore a large step-down change in marker spacing should be avoided in order to keep the system within an oscillatory limit. The system, operating at 0.50 damping ratio, subjected to a step change in marker spacing of 30 per cent gives a maximum overshoot of 2.75 per cent.

The compared simulation results of the linear and non-linear system in Figure 18 through 23 show that the linear response is the average of the non-linear one. More accuracy of approximation of the linear to the non-linear system results for lower values of marker spacing and controller gain; this because smaller force increments are applied to the vehicle. At higher damping ratios the linear system shows more deviation of the transient response from the non-linear system than at lower damping ratios. The speed of response during the transient stage of the linear system at high damping ratios is slower than the non-linear one. The overshoots are corrected rapidly.

To select the range of applicability of this particular feedback control system, the points of reducing high acceleration or deceleration, speed of response, the accuracy of approximation of the linear to the non-linear system, and small overshoots or undershoots, are considered. The desired range falls between damping ratios of 0.50 to 0.80 with the corresponding ratios of marker spacing to controller gain of 1 to 2.56 and a step change in marker spacing of 30 per cent.

APPENDICES

APPENDIX A
ANALOG COMPUTER SYMBOLS

THE FOLLOWING SYMBOLS ARE USED IN THE ANALOG COMPUTER PROGRAM

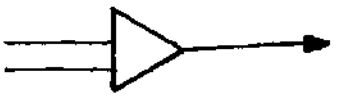

INVERTER OR SUMMER

INTERGRATOR

MULTIPLIER

DIVIDER

POTENTIO–MULTIPLIER

COMPARATOR

LOGICAL GATE

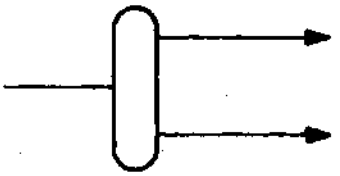

FLIP–FLOP

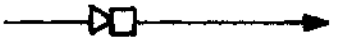

DRIVER

APPENDIX B

THE SKYBUS

General Description

The following information concerning the "skybus" is taken from the report on the Transit Expressway [7] developed and demonstrated at the South Park, Pittsburgh, Pennsylvania by the Westinghouse Electric Corporation.

The skybus is the electric vehicle, which resembles a bus and runs on four pairs of driven pneumatic tires. Operations are controlled by a central computer and electronic devices located on each vehicle and along the roadway. Each roadway has tracks which are 22" wide ribbons of concrete. A steel I-beam, called the guide beam, is mounted between these and is used by the guide wheels on the vehicle to steer each axle and to firmly position and lock the vehicle on the roadway. The propulsion power is supplied as three-phase alternating current to the trains and rectified on board each unit with silicon controlled rectifiers. Figure 24 shows the three-phase copper power rails which are mounted on brackets fastened to one of the track slabs. In the South Park project, power is supplied to the rails at a nominal voltage of 565 volts. A 300 KVA transformer provides all power to the system.

Spring-loaded current collectors are mounted on each axle assembly. The dual collectors insure continuity of power supply to the vehicle from the power rails. On board the vehicle a forced air cooled step-down transformer supplies

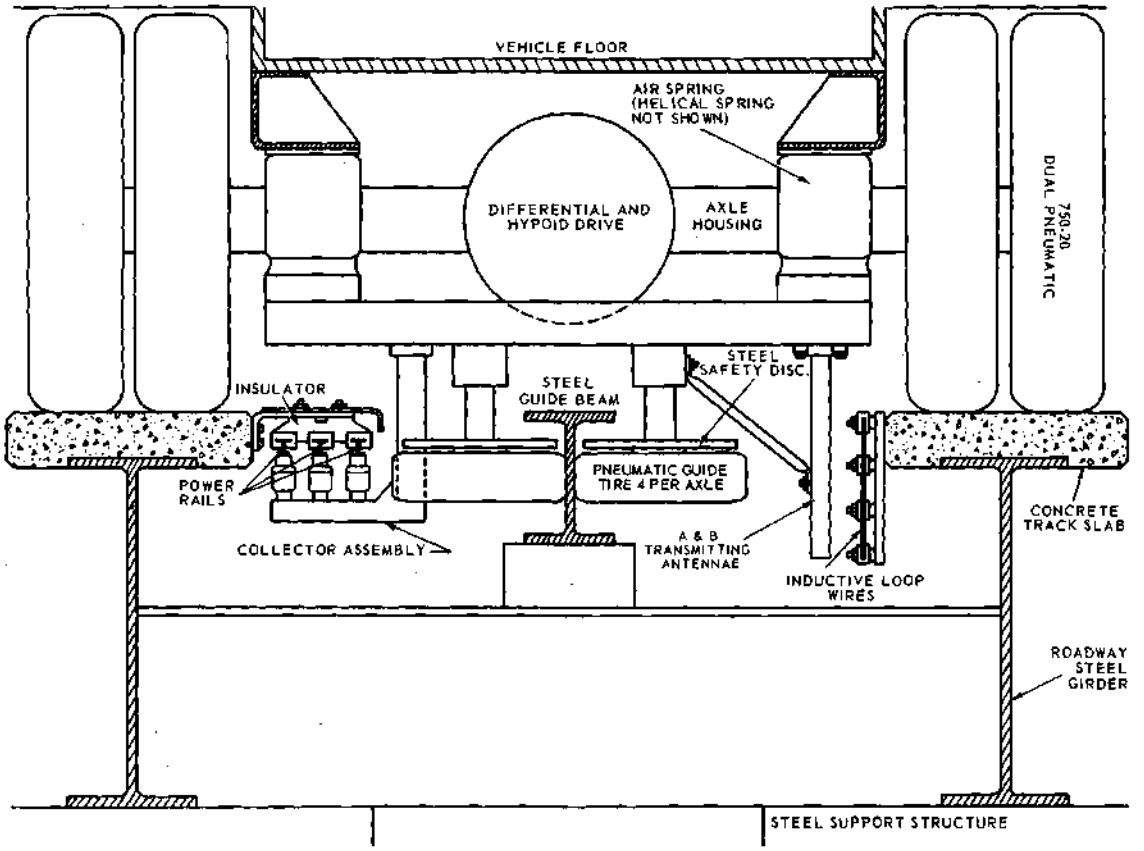

Figure 24. Arrangement of Vehicle Guidance, Power and Communication Equipment.

the alternating current power to the silicon controlled rectifiers which convert it to direct current for the two 60 horsepower propulsion motors.

Automatic Train Operation

The operation of all trains and vehicles in the South Park Transit Expressway is fully automatic requiring no operator or attendant on board. The heart of the control system is a Westinghouse PRODAC 550 electronic digital computer located at the North Station. This "wayside controller" monitors and controls the operation of the entire system.

The 9360 feet roadway is divided into nine sections or "control blocks" which are connected to the wayside controller at the North Station. For voice and command communications from the wayside controller to a train, each of the nine control blocks of roadway have a single insulated copper wire mounted parallel to the inside of the track slab. The ends of all nine of these straight wire inductive loops are connected by cable to the wayside controller. A second insulated copper wire for transmission of the A and B tones from the trains to the wayside controller is also mounted along the inside of the track slab in each of the nine control blocks. This is held in place by brackets in such a manner that the strand forms a square wave pattern 13 inches high, and vertical to the roadway surface. Between stations each wave is 15'3" long. In the vicinity of stations and other critical points, each square wave is one-eighth as long or 22-7/8" in order to give more precise control. The ends of all nine of the square wave inductive loops are connected by cable to the wayside controller as shown in Figure 25.

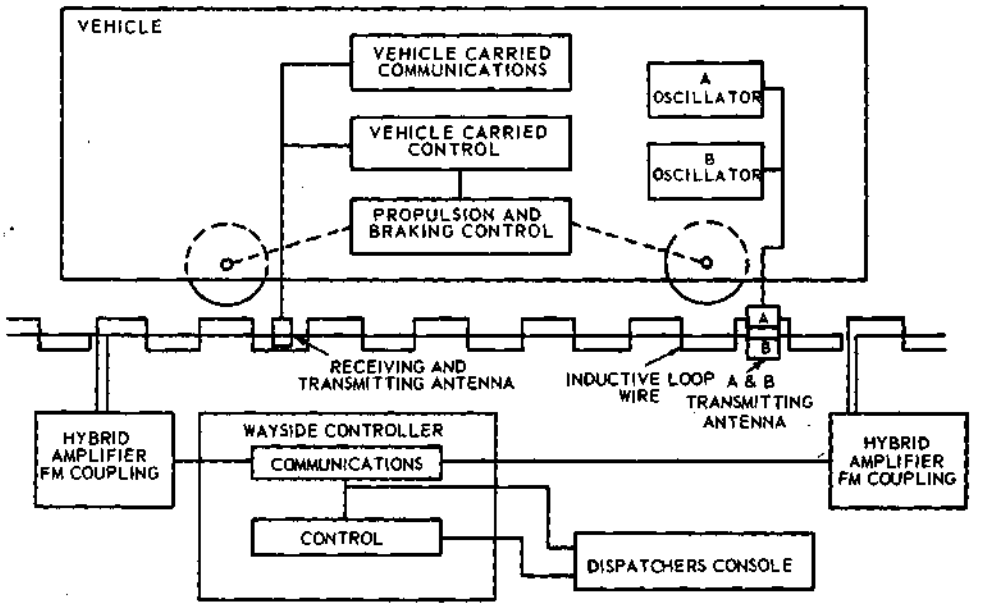

Figure 25. Block Diagram of Automatic Train Control System.

On board each vehicle are two oscillators which operate continuously at two different, but constant, frequencies. The "A" oscillator is connected to the upper coil of an antenna suspended below the vehicle. The "B" oscillator is similarly connected to the lower coil of the same antenna.

The wayside controller receives all information necessary to control the train from the two signals generated by the A and B oscillators. As the train moves along the roadway, the signal transmitted by the A antenna inductively couples with the top half of the square wave of the control block inductive loop wire and a strong A signal is received by the wayside controller. Since the coupling of the B antenna to the inductive loop wire is poor, a very weak B signal is received at the wayside controller.

As the train continues along the roadway, the coupling of the A and B antenna with respect to the inductive loop square wave reverses. Then, the wayside controller receives a strong B signal and a weak A signal. Thus, the A and B signals received at the wayside controller vary alternately in amplitude and provide A and B interrupt signals to the digital computer. When a train is comprised of only one vehicle, both the A and B oscillators are energized. If the train is comprised of several vehicles, the A oscillator operates on the lead and the B oscillator on the tail vehicle and all oscillators on the vehicles in between are deenergized.

The memory of the wayside controller contains information about each square wave in the inductive loop wires of each control block. The waves from the beginning of each inductive loop in a given control block are numbered. The

time (speed) to traverse each square wave is programmed on the basis of the roadway condition; i.e., straight track, curved track, station approach, station, or leaving a station.

As a train passes along the roadway, the wayside controller counts and times the A and B interrupts it receives, thus determining the exact location and speed of the train. The wayside controller determines train length from the difference between the A and B interrupt counts. The wayside controller compares the information received with the operating characteristics programmed in its memory for each specific square wave. Where the actual train performance varies from program or the instructions, the wayside controller determines the corrective measures necessary and transmits a command along the straight inductive loop wire to a receiving and transmitting communications antenna mounted beneath the vehicle. Only one train is tolerated in any given control block between any given time.

The wayside controller command to the vehicle is comprised of three separate and different audio tones transmitted simultaneously in the straight inductive loop wire. There are six separate audio tones for combination into the three tone commands, or twenty possible commands that can be transmitted to the train.

The receiving and transmitting communications antenna mounted beneath the vehicles and facing the straight inductive loop wire picks up the command signals transmitted by the wayside controller. On-board equipment receives the signals and checks to see that no more and no less than three tones are received. If the number varies, then on-board controls stop the train as a safety measure.

After checking the number of tones and their identity in the command signal, the reciever then outputs the command to propulsion motors, braking controls, or the door control as the case may be.

The wayside controller also continuously transmits a seventh command tone along the straight inductive loop wire several times per second. This tone is picked up by the train and serves to reset on-board circuits to prevent emergency braking. The wayside controller can bring any or all trains to an emergency stop by either discontinuing the normal seventh tone output, or outputting a continuous seventh tone. An eighth tone is provided, which, in conjunction with the other tones accomplishes the uncoupling of vehicles in the trains.

Comparison Between the Marker Counting System and the Skybus System

In the marker counting system the clock is used as reference pulse frequency. The frequency of the clock is constant during operation. The distance between the wayside markers are not equal except where the speed of the vehicle is required to be constant. These wayside markers generate pulse frequencies within each vehicle, which in turn are compared with the clock frequency through the bidirectional counter. The counter counts positively clock pulses and negatively wayside markers. The behavior of the vehicle is controlled by arranging the marker spacing. During steady state the two pulse frequencies are equal. The clock frequency and marker spacing determine the speed of the vehicle under control. The vehicle speed during steady state can be increased or decreased by making a

step change in marker spacing. A change in the clock frequency, however, changes the vehicle speed proportionally at all points along the guideway.

The skybus system uses the wayside markers which are evenly spaced. The spacings are closer in the vicinity where precise control is required. The reference pulse frequency is uneven. This is the information stored within the electronic digital computer or wayside controller according to how the vehicle behavior is desired. The counting of wayside markers is accomplished through the combination of two oscillators with different, but constant frequencies, and square wave inductive loop wire. As the vehicle moves along the guideway, the wayside controller counts and times the interrupts it receives, thus determining the exact location and speed of the vehicle. If the speed of the vehicle differs from that stored within the wayside controller, increase or decrease speed commands are sent to the vehicle, as the case may be.

The same scheme of counting the wayside markers can be used in the marker counting system by arranging square wave inductive loop wire so that it is unevenly spaced.

BIBLIOGRAPHY

1. Gordon D. Friedlander, Computer-controlled Vehicular Traffic, IEEE Spectrum, February 1969, p. 30-43.

2. W. S. Levine and M. Athans, On the Optimal Error Regulation of a String of Moving Vehicle, IEEE Transactions on Automatic Control, vol. AC-11, No. 3, July, 1966, p. 355-361.

3. Victor L. Streeter, Fluid Mechanics, Third Edition, p. 206, McGraw-Hill, 1962.

4. Harrison and Bollinger, Introduction to Automatic Controls, Fourth Edition, p. 69-70, International Textbook, 1968.

5. DiStefano III, Stubberud, Williams, Feedback and Control Systems, p. 362, Shaum Publishing Co., 1967.

6. Robert Blair Thornhill, Engineering Graphics and Numerical Control, p. vii-viii, p. 5, McGraw-Hill, 1967.

7. MPC Corporation, Pittsburgh, Transit Expressway Report, p. 11-17, Feb. 20, 1967.